Geometric Partial Differential Equations: Theory, Numerics and Applications

Organised by
Gerhard Dziuk, Freiburg
Charles M. Elliott, Warwick
Gerhard Huisken, Golm
Ralf Kornhuber, Berlin

November 27th – December 3rd, 2011

ABSTRACT. This workshop concentrated on partial differential equations involving stationary and evolving surfaces in which geometric quantities play a major role. Mutual interest in this emerging field stimulated the interaction between analysis, numerical solution, and applications.

Introduction by the Organisers

The workshop *Geometric partial differential equation: Theory, Numerics, and Applications*, organized by Gerd Dziuk (Freiburg), Charles M. Elliott (Warwick), Gerhard Huisken (Golm), and Ralf Kornhuber (Berlin) was held November 28–December 2, 2011. The scientific program consisted of 23 plenary talks with a good mix of slide and blackboard presentations and a 'Young researcher's session' on Wednesday evening. About 50 participants from America, Asia, and Europe represented the leading experts both from analysis and numerical analysis of partial differential equations (pdes) involving stationary and evolving surfaces and interfaces. The diversity of participants provided a wealth of new perspectives on this emerging field. Mutual interaction of analysis and numerics led to lively discussions after the talks, created a stimulating atmosphere throughout the conference, and gave rise to new, unexpected cooperations.

The focus was on partial differential equations of, on, and into *Stationary and evolving surfaces and interfaces.* Since the last decades of the preceding century,

mean curvature flow played a major role in geometric pdes. As one of the high-lights, Klaus Ecker reviewed fundamental results on the Cauchy problem in the graph case which, in contrast to the standard heat equation allows for a smooth solution for all times without any growth conditions. Matteo Novaga discussed the long-time behavior of mean curvature flow in heterogeneous media. Using variational arguments rather than maximum principles, he showed convergence to traveling wave solutions. Harald Garcke reported on existence results for clusters of hypersurfaces evolving by mean curvature that meet under suitable angle condi-tions. Many grains with boundaries moving by mean curvature were considered by Selim Esedoglu. His highly optimized level set algorithm allows for large scale sim-ulations of recrystallization for physically relevant parameter values. The motion of the interface of two immiscible fluids depends both on surface tension effects and on the dynamics in the bulk. Existence of strong solutions for an incom-pressible Navier-Stokes/Mullins-Sekerka system were presented by Helmut Abels. Anisotropic versions of mean curvature flow was considered by Carsten Gräser who concentrated on the stability analysis of various time discretizations of anisotropic phase field equations and the efficient and robust solutions of the resulting spa-tial problems by recent non-smooth Newton multigrid methods. Crystalline mean curvature flow is generated by anisotropic interfacial energies which are singular in the sense that the associated Frank diagram is no longer strictly convex. In his talk Yoshikazu Giga discussed polygonal motion, together with a variational and a viscosity approach to appropriate solution concepts and corresponding nu-merical techniques. Maurizio Paolini introduced the bidomain modell, a system of two reaction-diffusion equations, which turned out to be formally asymptotic to non-convex, anisotropic mean curvature flow, and presented some numerical experiments.

The notion of bending energy similar to classical Kirchhoff plate theory gives rise to Willmore or Hellfrich energies which play a significant role in the macro-scopic modeling of biomembranes. Klaus Deckelnick considered a conforming semi-discretization in space of the Willmore flow, i.e. the associated L^2 gradient flow of the Willmore energy in the graph case, and proved optimal error estimates for the resulting method of lines. Björn Stinner provided a numerical study of H^1-gradient flow for the Willmore functional using a mixed formulation consisting of quadratic and linear surface elements. A network of curves driven by elastic flow, a variant of Willmore flow, was considered by Robert Nürnberg. A striking feature of his algorithm is to use tangential motion to preserve well-distribution of mesh points throughout the evolution.

Ricci flow plays a crucial role not only in the celebrated proof of Poincaré's conjecture but also in general relativity. James Isenberg, one of the pioneers of this field, gave a survey on numerics, matched asymptotics, and analysis of degenerate neckpinches in Ricci flow, while Hans Fritz presented an innovative definition of discrete Ricci curvature on triangulated hypersurfaces of arbitrary dimension based on a suitable weak formulation.

Partial differential equations on surfaces. In spite of considerable progress during the last years, the numerical analysis of pdes on surfaces is still its infancy. The construction of parametrized cubical grids from an arbitrary tetrahedral mesh was presented by Konrad Polthier. Andrea Bonito reported on the state of the art of adaptive finite element methods for Laplace-Beltrami problems. Christian Lubich investigated implicit Runge-Kutta methods as applied to the ODEs arising from the spatially discrete Evolving Surface Finite Element Method. showing that the order of convergence is inherited from the classical case. Dietmar Kröner presented the ideas of a proof for existence and uniqueness of entropy solutions of nonlinear conservation laws on moving surfaces. Applications of adaptive finite elements to the numerical solution of the Einstein equations were given by Michael Holst. Oliver Rinne presented an approach to Einstein equations on constant mean curvature surfaces based on compactified coordinates. Many engineering problems involving, e.g., the motion of foams, grain growth or the evolution of multicellular structures give rise to coupled models for pdes of *and* on moving surfaces. James Sethian discussed a new appraoches to this class of problems and showed various applications.

Partial differential equations into surfaces. Partial differential equations with non-convex constraints often can be regarded as pdes into surfaces. For example, the elastic bending of a thin plate leads to a minimization problem with isometry constraints. Sören Bartels introduced and analyzed finite element appproximations of this problem and reported on recent numerical computations. Oliver Sander suggested an intrinsic approach to pdes into surfaces based on piecewise polynomial approximation along geodesics. An application of geodesic interpolation to topology preserving shape morphing and related problems in geometry processing were presented by Martin Rumpf.

The *Young researcher's session* on Wednesday evening took place in a relaxed athmosphere with a glass of wine provided by the organizers. Two PhD students and two post-docs took the opportunity to present their recent work to an international audience and discuss possible future developments and perspectives.

Workshop: Geometric Partial Differential Equations: Theory, Numerics and Applications

Table of Contents

Abstracts

Computing multiphase physics using the Voronoi Implicit Interface Method

JAMES A. SETHIAN

(joint work with Robert I. Saye)

Many scientific and engineering problems are characterized by a large number of different regions touching in many different configurations, and whose interaction depends on complex physics. Examples include the motions of foams, crystal grain growth, and multicellular structures in man-made and biological materials, as well as mathematical and computational problems, such as geometric motion, domain decomposition and surface area minimization problems.

It is challenging to produce consistent and well-posed mathematical models that accurately model the hydrodynamic, elastic, diffusive, and transport processes that often characterize such motions. Building robust numerical schemes is equally daunting, especially in the presence of multi-junction points (triple points, quadruple points, etc.) in 2D and the analogous structures in 3D, including triple lines where multiple surfaces meet, etc.

In this talk, we discuss a new set of computational methodologies [4, 5] to handle these problems. Our methods have several virtues. They use a single function on a fixed Eulerian mesh for an entire multiphase system, regardless of the number of phases, work in 2D/3D, and contain a real physical time that couples naturally to physics. The formulation automatically deals with the evolution of triple points/lines and topological change in the multiphase system, allowing phases to disappear and be created. The methods are first order accurate at triple points/lines, and arbitrarily high order away from these degeneracies. Finally, the methods have a computational complexity dependent only on the length of the interface.

Briefly, the method works as follows. Given a domain in $\mathbb{R}^n$, we imagine a collection of "phases" such that each point x in the domain is either in a unique phase, or on the boundary between two or more phases: this collection of boundaries will be known as the "interface". We define $\phi(x)$ as the distance from x to the closest point on the interface: this is the embedding of the interface as the zero level set of an *unsigned* distance function. We further assume that we are given a speed F defined on the interface, and create an "extension velocity" which defines a speed function $F_{ext}(x)$ in all of the domain, see [1].

The key idea is to note that a comparison theory ensures that the level set corresponding to the interface is embedded in a family of nearby level sets, and the motion of the zero level set corresponding to the interface is thus bracketed by the motion of surrounding level sets. While the interface where multiple phases touch may have high order junctions such as triple points and triple lines, the ϵ-level sets are hypersurfaces which exist solely in a single phase and do not contain such degeneracies.

We utilize this property to construct the VIIM. We first evolve the unsigned level set function according to the standard initial value PDE $\phi_t + F|\nabla\phi| = 0$ [3, 7]. Using the nearby ϵ-level sets, we then find the Voronoi diagram, which we then define as the new interface. We then reconstruct the unsigned distance function from this Voronoi construction. By making use of Chopp's bicubic reconstruction technique [6, 2], both the Voronoi construction and the rebuilding of the unsigned distance function can be done without ever explicitly constructing the interface.

Figure 1a shows the motion of a large number of connected phases undergoing curvature flow in which each phase maintains its own area while moving to minimize the total perimeter. Figure 1b/c shows multi-phase interactions under a large shear incompressible Navier-Stokes flow with surface tension and computed with and without permeability. Our methods are applicable across a range of multi-scale/multi-physics problems.
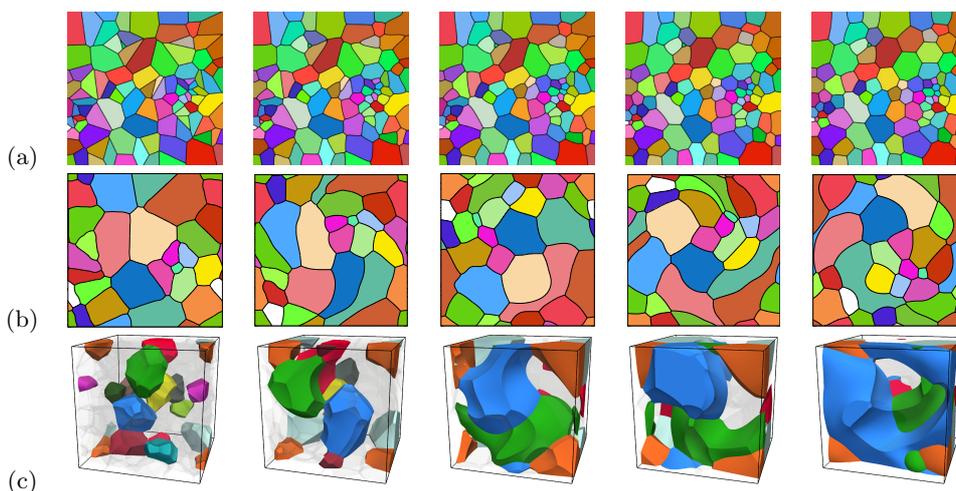
FIGURE 1. In all cases, time advances from left to right. (a) Curvature flow with area conservation on 100 initial ran dom phases. (b) Navier-Stokes fluid flow simulation with an external agitator force and no permeability. (c) Navier-Stokes 3D fluid flow with surface tension and permeability (subset of phases shown).

REFERENCES

[1] Adalsteinsson, D., and Sethian, J.A., *A* Fast Level Set Method for Propagating Interfaces, J. Comp. Phys., 118, 2, pp. 269–277, 1995.
[2] Chopp, D.L. *Some Improvements of the Fast Marching Method* SIAM Journal Scientific Computing, 23, 1, 2001.
[3] Osher, S., and Sethian, J.A., *Fronts Propagating with Curvature-Dependent Speed: Algorithms based on Hamilton-Jacobi Formulations*, J. Comp. Phys., 79, pp.12-49, (1988).

[4] Saye, R. and Sethian, J.A., *The Voronoi Implicit Interface Method for Computing Multi-phase Physics*, Proceedings of the National Academy of Sciences, published on-line, Nov. 21, 2011.

[5] Saye, R. and Sethian, J.A., *Analysis and Applications of the Voronoi Implicit Interface Method*, submitted for publication, Nov. 2011, Journal Computational Physics.

[6] Sethian, J.A., *A Fast Marching Level Set Method for Monotonically Advancing Fronts*, Proc. Nat. Acad. Sci., 93, 4, pp.1591–1595, 1996.

[7] Sethian, J.A., *Level Set Methods and Fast Marching Methods*, Cambridge Univ. Press, 1999.

Crystalline curvature flow with spatially inhomogeneous driving force

Yoshikazu Giga

1. Background

A crystalline curvature flow is a typical anisotropic curvature flow whose interfacial energy is convex but singular. A typical example of anisotropic curvature equation is of form

$$(1) \qquad V = M(\mathbf{n})(\kappa_\gamma + \sigma) \quad \text{on} \quad \Gamma_t$$

for a closed evolving hypersurface $\{\Gamma_t\}_{t \geq 0}$ in $\mathbf{R}^d$, where V is the normal velocity in the direction of unit normal vector field $\mathbf{n}$ of Γ_t. Here κ_γ is an anisotropic mean curvature with an interfacial energy density γ; $M(\mathbf{n}) > 0$ is a mobility while σ is a driving force term. The interfacial energy density γ is assumed to be a convex, positively 1-homogeneous function in $\mathbf{R}^d$. The anisotropic mean curvature is formally defined by $\kappa_\gamma = -\text{div}_{\Gamma_t} \xi(\mathbf{n})$, $\xi(\mathbf{n}) = \nabla_p \gamma(\mathbf{n})$, where div_{Γ_t} is the surface divergence [9, Chapter 1].

We are interested in the case when γ is NOT C^1 in $\mathbf{R}^d \backslash \{0\}$ nor strictly convex in the sense γ^2 is strictly convex (which is equivalent to say that 1-level set of γ (Frank diagram) is strictly convex; see e.g. [9, Chapter 1].) A typical example of such an energy density is the case when γ is piecewise linear so that its Frank diagram is polytope. In this case the flow (1) is called a *crystalline flow* and the interfacial energy density γ is called a crystalline energy. When (1) is a planar motion, i.e. $d = 2$, then κ_γ is written as $\kappa_\gamma = \left(\bar{\gamma}''(\theta) + \bar{\gamma}(\theta)\right)\kappa$ with $\bar{\gamma}(\theta) = \gamma(\cos\theta, \sin\theta)$, $\mathbf{n} = (\cos\theta, \sin\theta)$, where κ is the usual curvature. If γ is a crystalline interfacial energy, $\bar{\gamma}'' + \bar{\gamma} = \Sigma_{k=1}^m c_k \delta(\theta - \theta_k)$, $c_k > 0$. From a view point of partial differential equations the crystalline flow equation (1) is degenerate parabolic for $\theta \neq \theta_k$ while the diffusion effect at $\theta = \theta_k$ is so strong that it is nonlocal. Thus such an equation is often called very singular parabolic equations; see [7] for a review including higher order equations.

The notion of solutions so that its initial value prolem is well-posed (i.e. solving $\{\Gamma_t\}$ with given initial data Γ_0) is highly nontrivial. There are at least three approaches.

1. (Finding a special class preserved by flow.) One restricts the class of solutions into a special class of polygonal motion which works well when $d = 2$ and σ is spatially constant for crystalline flow [1], [11]. However, it

is impossible to extend this idea for $d \geq 3$ so that a flow enjoys comparison principle [3] although a similar motion for polyhedra itself is well-posed [10]. The merit of this approach is that the problem is reduced to a system of ordinary differential equations.

2. (Variational approach.) A conventional way is to apply a nonlinear semi-group theory which applies for the graph-like solutions for $d = 2$ when $\sigma \equiv 0$ [4]. Later, using distance function a notion of solution for $d \geq 2$ when $\sigma \equiv 0$ and $M = \gamma$ is introduced so that a comparison principle is fulfilled. However, the existence of solution is known only for convex initial data; see [2] and papers cited there. Here γ can be more general than crystalline.

3. (Viscosity approach.) One extends the theory of viscosity solutions for a nonlocal diffusion equation, which is highly nontrivial. Fortunately, for graph-like solutions such a theory is established in the case of planar motion when σ is spatially constant [5]. A level set method for a closed value is also established [6]. This approach is flexible in the sense that one can handle a more general flow than (1) in the sense the curvature dependence of the right hand side may be nonlinear, say $|\kappa_\gamma|^\alpha \kappa_\gamma$, $\alpha > 0$. Moreover, γ can be more general than crystalline.

2. FEATURE OF RESULTS

Jointly with Mi-Ho Giga (Tokyo) and Piotr Rybka (Warsaw) [8] we are able to extend the theory of viscosity solutions for $d = 2$ and for graph-like solutions when σ is spatially inhomogeneous. A key issue is a comparison of curvature like quantity on a flat part called a fecet as well as its stability with respect to a facet. Here is a typical example.

$$(2) \qquad u_t = a(u_x)\left[(\operatorname{sgn} u_x)_x + \sigma(x)\right], \ a > 0$$

Some classes of crystalline curvature flow (1) deduces (2) when $\Gamma_t = \{y = u(x,t), x \in \mathbf{R}\}$. If $u_x \neq 0$, then (2) is reduced to $u_x = a(u_x)\sigma(x)$. At the place where $u_x = 0$ the solution u feels very strong diffusion. To motivate the speed we consider the profile v so that v takes its minimal value 0 on (a,b) and $v > 0$ outside (a,b). It turns out that the natural quantity for $\Lambda = (\operatorname{sgn} u_x)_x + \sigma(x)$ on (a,b) is

$$(3) \qquad \Lambda = \eta_x^0(x) + \sigma(x)$$

$$(4) \qquad \eta^0(x) = \arg\min\left\{\int_a^b |\eta_x + \sigma|^2 \mathrm{d}x \ \Big| \ |\eta(x)| \leq 1, \ \eta(a) = -1, \ \eta(b) = 1\right\}.$$

The problem (4) is an obstacle problem. If σ is constant, then the graph of η^0 is a straight line and its slope agrees with a crystalline curvature $2/(b-a)$. In this case η_x^0 is constant. However, this curvature like quantity Λ is not a constant in general so "a facet" may bend. Moreover, it is not a sum of a crystalline curvature and σ. Neverthless, we are able to establish a comparison principle for Λ and elaborating

a method developed by [5]. In particular, we are able to prove the comparison principle for suitably defined viscosity solutions.

Equations with singular diffusion are not restricted just for a crystalline flow in materials science. It is also popular as a total variation flow in image processing $u_t = \mathrm{div}\big(\nabla u/|\nabla u|\big)$. Except one variable case a facet may break even if there is no inhomogenerous driving force term. In our ongoing project (jointly with Mi-Ho Giga and Norvert Pozar (Tokyo)) we are trying to build a theory of viscosity solutions including

$$(5) \qquad u_t = a(\nabla u)\mathrm{div}\big(\nabla u/|\nabla u|\big)$$

with $a \geq 0$ by defining a nonlocal speed in a reasonable way. Note that a nonlinear semigroup theory does not apply for (3) (unless a is a constant) so other than our approach it was not clear that whether or not the initial value problem (3) is well-posed.

References

[1] S. B. Angenent and M. E. Gurtin, *Multiphase thermomechanics with interfacial structure, 2. Evolution of an isothermal interface*, Arch. Rational. Mech. Anal. **108** (1989), 323–391.

[2] G. Bellettini, V. Caselles, A. Chambolle and M. Novaga, *Crystalline mean curvature flow of convex sets*, Arch. Ration. Mech. Anal. **179** (2006), 109–152.

[3] G. Bellettini, M. Novaga and M. Paolini, *Facet-breaking for three dimensional crystals evolving by mean curvature*, Interfaces Free Bound. **1** (1999), 39–55.

[4] T. Fukui and Y. Giga, *Motion of a graph by nonsmooth weighted curvature*, In: World Congress of Nonlinear Analysis '92 (ed. V. Lakshmikantham), Walter de Gruyter, Berlin **1** (1996), 47–56.

[5] M.-H. Giga and Y. Giga, *Evolving graphs by singular weighted curvature*, Arch. Ration. Mech. Anal. **141** (1998), 117–198.

[6] M.-H. Giga and Y. Giga, *Generalized motion by nonlocal curvature in the plane*, Arch. Rational. Mech. Anal. **159** (2001), 295–333.

[7] M.-H. Giga and Y. Giga, *Very singular diffusion equations - second and fourth order problems*, Japanese J. Indust. Appl. Math. **27** (2010), 323–345.

[8] M.-H. Giga, Y. Giga and P. Rybka, *A comparison principle for singular diffusion equations with spatially inhomogeneous driving force for graphs*, Hokkaido University Preprint Series for Mathematics, ♯ **981** (2011).

[9] Y. Giga, *Surface Evolution Equations - A level set approach*, Birkhäuser, Basel (2006).

[10] Y. Giga, M. E. Gurtin and J. Matias, *On the dynamics of crystalline motion*, Japanese J. Indust. Appl. Math. **15** (1998), 7–50.

[11] J. Taylor, *Constructions and conjectures in crystalline nondifferential geometry*, In: Differential Geometry (ed. B. Lawson and K. Tanenblat), Proceedings of the Conference on Differential Geometry, Rio de Janeiro, Pitman Monographs Surveys in Pure and Applied Math. **52** (1991) 321–336.

Approximation of the Willmore flow of graphs by C^1–finite elements

Klaus Deckelnick

(joint work with Friedhelm Schieweck)

Let $\Omega \subset \mathbb{R}^2$ be a bounded domain with a smooth boundary. For a smooth function $u : \bar{\Omega} \to \mathbb{R}$ we consider its graph $\Gamma = \{(x, u(x)) \,|\, x \in \bar{\Omega}\}$, whose mean curvature is given by

$$H = \frac{1}{2} \nabla \cdot \Big(\frac{\nabla u}{\sqrt{1 + |\nabla u|^2}} \Big) = \frac{1}{2} \frac{1}{\sqrt{1 + |\nabla u|^2}} \sum_{i,j=1}^{2} \Big(\delta_{ij} - \frac{u_{x_i} u_{x_j}}{1 + |\nabla u|^2} \Big) u_{x_i x_j}.$$

Hence, the Willmore functional $W(\Gamma) = \dfrac{1}{2} \displaystyle\int_{\Gamma} H^2 dS$ can be written in terms of u as follows:

$$(1) \qquad W(u) = \frac{1}{2} \int_{\Omega} H^2 \sqrt{1 + |\nabla u|^2} dx = \frac{1}{2} \int_{\Omega} [E(\nabla u) : D^2 u]^2 dx,$$

where the colon denotes the usual inner product for matrices and $E : \mathbb{R}^2 \to \mathbb{R}^{2 \times 2}$ is given by

$$E(p)_{ij} = \frac{1}{4} (1 + |p|^2)^{-\frac{1}{4}} \Big(\delta_{ij} - \frac{p_i p_j}{1 + |p|^2} \Big), \quad i, j = 1, 2, p \in \mathbb{R}^2.$$

We are interested in calculating local or global minima of W subject to Dirichlet boundary conditions. To do so, we consider the evolution of a family of graphs $\Gamma(t) = \{(x, u(x, t)) \,|\, x \in \bar{\Omega}\}$ by the L^2–gradient flow of W, the so–called Willmore flow. Since the normal velocity of $\Gamma(t)$ is given by $V = \frac{u_t}{\sqrt{1 + |\nabla u|^2}}$ we obtain the following variational formulation for this evolution:

$$(2) \quad \int_{\Omega} \frac{u_t(\cdot, t)\phi}{\sqrt{1 + |\nabla u(\cdot, t)|^2}} dx + \langle W'(u(\cdot, t), \phi \rangle = 0 \qquad \text{for all } \phi \in H_0^2(\Omega), t \in (0, T]$$

$$(3) \qquad\qquad u(\cdot, t) = g, \quad \frac{\partial u}{\partial \nu}(\cdot, t) = g_\nu \qquad \text{on } \partial\Omega \times (0, T]$$

$$(4) \qquad\qquad\qquad\qquad u(\cdot, 0) = u_0 \qquad \text{in } \bar{\Omega}.$$

Here, $g, g_\nu : \partial\Omega \to \mathbb{R}$ and $u_0 : \bar{\Omega} \to \mathbb{R}$ are given functions. Note that

$$\langle W'(u), \phi \rangle = \int_{\Omega} E(\nabla u) : D^2 u \big\{ E(\nabla u) : D^2 \phi + \sum_{k=1}^{2} \phi_{x_k} E_{p_k}(\nabla u) : D^2 u \big\},$$

so that it follows from (2) that u satisfies a highly nonlinear parabolic PDE of fourth order. We approximate solutions of (2), (3), (4) with the help of C^1–finite elements. Let $(\mathcal{T}_h)_{h>0}$ be a sequence of exact triangulations of $\bar{\Omega}$, so that boundary elements are allowed to have one curved edge. For $T \in \mathcal{T}_h$ we consider the Hsieh-Clough-Tocher element

$$P(T) := \{p \in C^1(T) \,|\, p_{|T_i} \in P_3(T_i), i = 1, 2, 3\},$$

where T is subdivided into three triangles T_1, T_2, T_3 by joining the barycenter of T to its vertices. We emphasize that also for boundary elements $p_{|T_i}$ is a cubic polynomial in the original coordinates, so that we do not use the iso-parametric finite element concept. We now define $X_h \subset H^2(\Omega)$ by

$$X_h := \{\phi_h \in C^1(\bar{\Omega}) \,|\, \phi_{h|T} \in P(T), T \in \mathcal{T}_h\}.$$

Furthermore, the space X_{h0} consists of those $\phi_h \in X_h$, for which the boundary degrees of freedom vanish, i.e if e is a boundary edge with vertices a_1, a_2 and midpoint b (with respect to arclength), we require that $\phi_h(a_i) = 0, \nabla \phi_h(a_i) = 0, i = 1, 2$ and $\frac{\partial \phi_h}{\partial \nu}(b) = 0$. Note that in general $X_{h0} \not\subset H_0^2(\Omega)$, so that it is crucial to estimate boundary integrals involving functions in X_{h0}. Such estimates have been derived in [5] even for more general C^1–finite element spaces.

The semi–discrete problem now reads: Find $u_h : \bar{\Omega} \times [0, T] \to \mathbb{R}$ such that $u_h(\cdot, t) \in X_h$ for all $t \in [0, T], u_h(\cdot, 0) = u_{h0}$ in Ω and

$$\int_\Omega \frac{u_{ht}(\cdot, t)\phi_h}{\sqrt{1 + |\nabla u_h(\cdot, t)|^2}} dx + \langle W'(u_h(\cdot, t), \phi_h \rangle = 0 \quad \text{for all} \ \ \phi_h \in X_{h0}, t \in (0, T].$$

Here, $u_{h0} \in X_h$ is a suitable approximation of the initial datum u_0. The boundary degrees of freedom $u_h(\cdot, t)$ are determined in terms of g and g_ν. Our main result is the following error estimate.

Theorem *Suppose that $u : \bar{\Omega} \times [0, T] \to \mathbb{R}$ is a smooth solution of (2), (3), (4). Then there exists $h_0 > 0$ such that for $0 < h \leq h_0$ the semi–discrete solution u_h exists on $\bar{\Omega} \times [0, T]$ and satisfies*

$$\left(\int_0^T \|u_t - u_{ht}\|_{L^2}^2 dt\right)^{\frac{1}{2}} + \max_{t \in [0,T]} \|(u - u_h)(\cdot, t)\|_{H^2} \leq Ch^2.$$

A corresponding analysis in the case of rotationally symmetric surfaces is given in [4]. Since the implementation of C^1–finite elements is rather complicated, much of the previous work on the discretisation of Willmore flow was carried out in the framework of C^0–elements. This is possible by splitting the fourth order problem into two second order problems via the introduction of a second variable which is usually related to the mean curvature. In the case of graphs and level sets evolving by Willmore flow such a method was developed in [6] and an error analysis for the flow of graphs subject to Navier boundary conditions can be found in [3]. Similar approaches using finite differences and a discontinuous Galerkin-method can be found in [8] and [10] respectively. Splitting methods for the evolution of parametric surfaces by Willmore flow and related geometric evolution laws have been developed in [7], [1], [2] and [9].

References

[1] J.W. Barrett, H. Garcke, R. Nürnberg, Parametric approximation of Willmore flow and related geometric evolution equations, *SIAM J. Sci. Comp.* **31**, 225–253 (2008).

[2] A. Bonito, R.H. Nochetto, M.S. Pauletti, Parametric FEM for geometric biomembranes, *J. Comput. Phys.* **229**, 3171–3188 (2010).

[3] K. Deckelnick, G. Dziuk, Error analysis of a finite element method for the Willmore flow of graphs, *Interfaces Free Bound.* **8**, 21-46 (2006).

[4] K. Deckelnick, F. Schieweck, Error analysis for the approximation of axisymmetric Willmore flow by C^1-elements, *Interfaces Free Bound.* **12**, 551-574 (2010).

[5] J. Douglas Jr., T. Dupont, P. Percell, R. Scott, A family of C^1–finite elements with optimal approximation properties for various Galerkin methods for 2nd and 4th order problems, *RAIRO Anal. Numer.* **13**, 227-255 (1979).

[6] M. Droske, M. Rumpf, A level set formulation for Willmore flow, *Interfaces Free Bound.* **6**, 361-378 (2004).

[7] G. Dziuk, Computational parametric Willmore flow, *Numer. Math.* **111**, 55-80 (2008).

[8] T. Oberhuber, Finite difference scheme for the Willmore flow of graphs, *Kybernetika* **43**, 855-867 (2007).

[9] N. Olischläger, M. Rumpf, Two step time discretization of Willmore flow, Edwin R. Hancock, Ralph R. Martin, Malcolm A. Sabin (Eds.): Mathematics of Surfaces XIII, 13th IMA International Conference, York, UK, September 7-9, 2009, 278–292, Proceedings. Lecture Notes in Computer Science 5654, Springer (2009).

[10] Y. Xu, C.-W. Shu, Local discontinuous Galerkin method for surface diffusion and Willmore flow of graphs, *J.Sci. Comput.* **40**, 375–390 (2009).

Geometric evolution equations with triple junctions in higher dimensions

HARALD GARCKE

(joint work with Daniel Depner, Yoshihito Kohsaka)

Motion by mean curvature for evolving hypersurfaces in $\mathbb{R}^{d+1}$ is given by

$$V = H$$

where V is the normal velocity and H is the mean curvature of the evolving surface. Mean curvature flow for closed surfaces is the L^2-gradient flow of the area functional and many results for this flow have been established over the last 30 years.

Less is known for mean curvature flow of surfaces with boundaries. In the simplest cases one either prescribes fixed Dirichlet boundary data or one requires that surfaces meet a given fixed surface with a 90 degree angle. The last situation can be interpreted as the L^2-gradient flow of area taking the side constraint into account that the boundary of the surface has to lie on a given external surface. Local well posedness in this case was shown by Stahl [12] who was also able to formulate a continuation criterion. In addition he showed that surfaces converge asymptotically to a half sphere before they vanish.

Much less is known about the gradient flow dynamics for surface clusters. In this case hypersurfaces $\Gamma^1, \ldots, \Gamma^N$ in $\mathbb{R}^{d+1}$ with boundaries $\partial\Gamma^1, \ldots, \partial\Gamma^N$ meet at $(d-1)$-dimensional triple junctions, see e.g. Figure 1. Here, boundary conditions at the triple junction which can be derived variationally have to be described. In what follows we briefly discuss how to derive these boundary conditions. We define
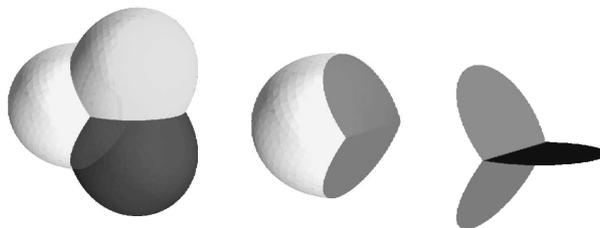
FIGURE 1. A triple bubble

the weighted surface free energy

$$\mathcal{F}(\Gamma) := \sum_{i=1}^{N} \int_{\Gamma^i} \gamma^i d\mathcal{H}^d$$

for a given surface cluster $\Gamma = (\Gamma^1, \ldots, \Gamma^N)$ (and constant surface energy density $\gamma_i > 0$) and consider a given smooth vector field

$$\zeta : \mathbb{R}^{d+1} \to \mathbb{R}^{d+1}.$$

Then we can define a variation $\Gamma(\varepsilon)$ of Γ in the direction ζ via

$$\Gamma^i(\varepsilon) = \{x + \varepsilon\zeta(x) \mid x \in \Gamma^i\}.$$

A transport theorem now gives

$$\frac{d}{d\varepsilon} \int_{\Gamma^i} 1 d\mathcal{H}^d = -\int_{\Gamma^i} V^i H^i + \int_{\partial\Gamma^i} v^i$$

where V^i is the normal velocity and H^i is the mean curvature of Γ^i. In addition v^i is the outer conormal velocity of the surface (for details we refer to Depner and Garcke [6] and Depner [5]).

The complete first variation is now given by

$$\frac{d}{d\varepsilon} \mathcal{F}(\Gamma(\varepsilon)) = \sum_i \int_{\Gamma^i(\varepsilon)} -\gamma^i V^i H^i d\mathcal{H}^d + \sum_i \int_{\partial\Gamma^i(\varepsilon)} \gamma^i v^i d\mathcal{H}^{d-1}$$

and hence the L^2-gradient flow is given by

(1) $$V^i = \gamma^i H^i \qquad \text{on } \Gamma^i \text{ and}$$

(2) $$\sum_{i=1}^{3} \gamma^i \tau^i = 0 \qquad \text{at triple junctions,}$$

where τ^i is the unit outer conormal of $\partial\Gamma^i$. We remark that the last condition reduces to a 120° angle condition in the case that all γ_i's are equal.

Local well-posedness for curves in the plane has been shown by Bronsard and Reitich [4] in a $C^{2+\alpha, 1+\frac{\alpha}{2}}$ setting using parabolic regularity theory and a fixed point argument (for a typical solution see Figure 2).

equal area   non-equal area
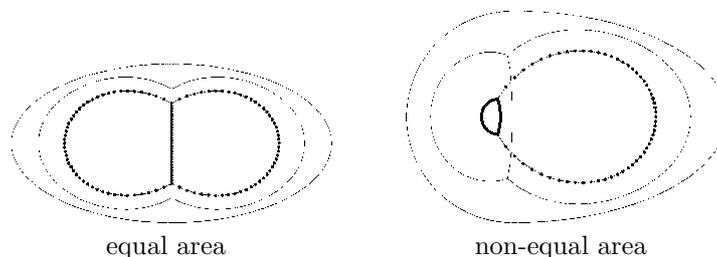
FIGURE 2. Mean curvature flow of a double bubble in the plane, see [2] for results in $\mathbb{R}^3$.

Mantegazza, Novaga and Tortorelli [10] were able to establish continuation criteria and Schnürer et al. [11] considered the asymptotic behaviour of lens-shaped geometries.

The higher dimensional situation is much more involved as the triple junction now is at least one-dimensional and a tangential degree of freedom arises. In addition all mathematical descriptions of the problem result in formulations which lead to a free boundary problem. Only recently Freire [8] was able to show local well-posedness in the case of graphs. Of course most situations cannot be represented as graphs. We use a new parametrization of surface clusters introduced in Depner and Garcke [6] to state the problem (1), (2) as a system of non-local, quasilinear parabolic partial differential equations of second order. The PDEs are defined on a surface cluster and are non-trivially coupled at the junctions. We are able to show the following result (for a precise formulation of the theorem we refer to [7]):

Theorem (Depner, Garcke, Kohsaka, 2011)

Let $(\Gamma_0^1, \Gamma_0^2, \Gamma_0^3)$ be a $C^{3+\alpha}$ surface cluster with a $C^{3+\alpha}$ triple junction curve γ. We assume the compatibility conditions

- *$(\Gamma_0^1, \Gamma_0^2, \Gamma_0^3)$ fulfill the angle conditions,*
- *$H_0^1 + H_0^2 + H_0^3 = 0$.*

Then there exists a local $C^{2+\alpha, 1+\frac{\alpha}{2}}$ solution of

$$V^i = H^i$$

$$+ angle\ conditions,$$

with initial data $(\Gamma_0^1, \Gamma_0^2, \Gamma_0^3)$.

The idea of the proof is as follows:

- Study the linearized problem with energy methods (this is nontrivial as the system is defined on a surface cluster).
- Show local $C^{2+\alpha, 1+\frac{\alpha}{2}}$-regularity of the solutions to the linearized problem. In order to apply classical regularity theory close to the triple junction, we parametrize the cluster locally over one fixed reference domain and

check the Lopatinski-Shapiro condition for the resulting system on the flat reference domain with an energy argument.
- Use a fixed point argument in $C^{2+\alpha,1+\frac{\alpha}{2}}$ which is non-trivial as the overall system is non-local. In this context ideas of Baconneau and Lunardi [1] are useful.

References

[1] O. Baconneau, A. Lunardi, *Smooth solutions to a class of free boundary parabolic problems*, Trans. Amer. Math. Soc. **356** (2004), no. 3, 987–1005.

[2] J.W. Barrett, H. Garcke, R. Nürnberg, *Parametric approximation of surface clusters driven by isotropic and anisotropic surface energies*, Interfaces Free Boundaries **12** (2010), no. 2, 187–234.

[3] K.A. Brakke, *The Motion of a Surface by its Mean Curvature*, Math. Notes **20**, Princeton Univ. Press, Princeton, NJ (1978).

[4] L. Bronsard, F. Reitich, *On three-phase boundary motion and the singular limit of a vector valued Ginzburg–Landau equation*, Arch. Ration. Mech. Anal. **124** (1993), 355–379.

[5] D. Depner, *Stability Analysis of Geometric Evolution Equations with Triple Lines and Boundary Contact*, Dissertation, Regensburg 2010.

[6] D. Depner, H. Garcke, *Linearized stability analysis of surface diffusion for hypersurfaces with triple lines*, Preprint no. 15 (2011), University Regensburg, to appear in Hokkaido Mathematical Journal.

[7] D. Depner, H. Garcke, Y. Kohsaka, *Mean curvature flow with triple junctions in higher space dimensions*, in preparation.

[8] A. Freire, *Mean curvature motion of triple junctions of graphs in two dimensions*, Comm. Partial Differential Equations **35** (2010), no. 2, 302–327.

[9] H. Garcke, Y. Kohsaka, D. Ševčovič, *Nonlinear stability of stationary solutions for curvature flow with triple junction*, Hokkaido Math. J. **38** (2009), no. 4, 721–769.

[10] C. Mantegazza, M. Novaga, V.C. Tortorelli, *Motion by curvature of planar networks*, Ann. Sc. Norm. Super. Pisa Cl. Sci. (5) **3** (2004), no. 2, 235–324.

[11] O.C. Schnürer, A. Azouani, M. Georgi, J. Hell, N. Jangle, A. Koeller, T. Marxen, S. Ritthaler, M. Sáez, F. Schulze, B. Smith, *Evolution of convex lens-shaped networks under the curve shortening flow*, Trans. Amer. Math. Soc. **363** (2011), no. 5, 2265–2294.

[12] A. Stahl, *Regularity estimates for solutions to the mean curvature flow with a Neumann boundary condition*, Calc. Var. Partial Differential Equations **4** (1996), no. 4, 385–407.

Evolution of the Einstein equations on constant mean curvature surfaces

Oliver Rinne

(joint work with Vincent Moncrief)

This report is concerned with the Einstein equations

$$(1) \qquad R_{ab} - \tfrac{1}{2} R g_{ab} = \kappa T_{ab},$$

where g_{ab} is a pseudo-Riemannian metric on a four-dimensional smooth manifold (spacetime), R_{ab} is its Ricci tensor (with respect to the Levi-Civita connection), and $R = g^{ab} R_{ab}$ is the scalar curvature. On the right-hand side, T_{ab} is the energy-momentum tensor describing the matter content of spacetime.

Here we are interested in solutions to (1) describing *isolated systems*: a compact source surrounded by an asymptotically flat vacuum spacetime. It is useful to introduce [1] a conformally related metric $\tilde{g}_{ab}$ via

$$(2) \qquad\qquad\qquad\qquad g_{ab} = \Omega^{-2}\tilde{g}_{ab}.$$

In suitably compactified coordinates, spacetime occupies a finite region, $\tilde{g}_{ab}$ is finite everywhere with respect to these coordinates, and the conformal factor Ω vanishes on the conformal boundary. This can be illustrated by a *Penrose diagram* (Fig. 1).

The standard approach to solving (1) numerically is to foliate spacetime into spacelike hypersurfaces approaching spacelike infinity i^0 (left panel of Fig. 1). These are truncated at a finite distance, where suitable boundary conditions must be imposed such that the resulting initial-boundary value problem is well posed and, ideally, spurious reflections of gravitational radiation are avoided. However, gravitational radiation is only defined unambiguously at future null infinity $\mathscr{I}^+$. Thus it would be very desirable to include $\mathscr{I}^+$ in the computational domain. We do this by considering instead *hyperboloidal* slices that are everywhere spacelike but approach $\mathscr{I}^+$ (right panel of Fig. 1). More specifically, we choose hypersurfaces that have constant mean curvature; in the following $K > 0$.

Throughout we work with the conformal metric in compactified coordinates. Instead of Friedrich's regular conformal field equations [2], we work directly with (a $3+1$ reduction of) the Einstein equations, mainly because these are the equations that numerical relativists have more experience with. The drawback of this approach is that the equations contain terms with negative powers of the conformal factor Ω that become singular at $\mathscr{I}^+$.

In particular, the evolution equation for the traceless part of the momentum π^{ij} conjugate to the induced spatial conformal metric γ_{ij} on the $t = \text{const}$ slices takes the form

$$(3) \qquad \partial_t \pi^{\mathrm{tr}\, ij} = -2\tilde{N}\Omega^{-1}(\tfrac{1}{3}K\pi^{\mathrm{tr}\, ij} + \mu_\gamma \mathrm{Hess}\, \Omega^{\mathrm{tr}\, ij}) + (\text{regular}),$$

where tr denotes the tracefree part with respect to γ_{ij}, $\tilde{N}$ is the conformal lapse function, $\mu_\gamma = \sqrt{\det \gamma_{ij}}$, and Hess denotes the Hessian with respect to γ_{ij}. The constraint equations that hold within the $t = \text{const}$ slices are also formally singular at $\mathscr{I}^+$. For instance, the Hamiltonian constraint reads

$$(4) \qquad -4\Omega\gamma^{ij}\tilde{\nabla}_i\tilde{\nabla}_j\Omega + 6\gamma^{ij}\Omega_{,i}\Omega_{,j} - \Omega^2\tilde{R} - \tfrac{2}{3}K^2 + \Omega^2\mu_\gamma^{-2}\gamma_{ik}\gamma_{jl}\pi^{\mathrm{tr}\, ij}\pi^{\mathrm{tr}\, kl} = 0,$$

where $\tilde{\nabla}$ is the covariant derivative of γ_{ij} and $\tilde{R}$ is its Ricci scalar. This singular form of the elliptic constraint equations works in our favour here because we can use it in order to determine the leading-order behaviour of the fields near $\mathscr{I}^+$. This will then allow us to evaluate the formally singular terms in (3).

On a given spatial slice, we choose coordinates such that the conformal boundary is given by $x^1 \equiv r = r_+$, where r_+ is a constant. We expand the fields in finite Taylor series about $r = r_+$ and substitute the expansions in the singular elliptic equations. For example, the Hamiltonian constraint (4) yields expressions for the first three radial derivatives of Ω at $\mathscr{I}^+$. A similar procedure is applied to the
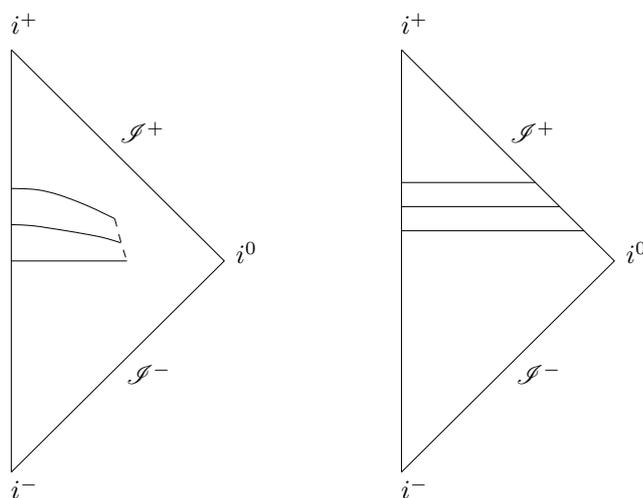
FIGURE 1. Cauchy evolution with timelike boundary (left) vs. hyperboloidal evolution (right). As an example, the Penrose diagram of flat (Minkowski) spacetime is shown. The conformal boundary consists of future and past null infinity ($\mathscr{I}^+$ and $\mathscr{I}^-$), future and past timelike infinity (i^+ and i^-), and spacelike infinity i^0.

momentum constraints. Using this method we obtain manifestly regular expressions for the formally singular terms in (3). We also recover regularity conditions previously derived in [3], namely that the shear and the components $\pi^{\mathrm{tr}\,ri}$ of the traceless momentum must vanish at $\mathscr{I}^+$, and we show that these conditions are preserved under the time evolution. Further details can be found in [4].

A similar scheme to the one described above has been implemented numerically [5] under the assumption that spacetime is axisymmetric so that there are two effective spatial dimensions. The spatial coordinates are chosen such that the two-metric takes on a conformally flat form (quasi-isotropic gauge). The numerical method consists of fourth-order finite differences on a spherical polar grid, the method of lines with a fourth-order Runge-Kutta method for the time integration, and multigrid (FAS) for the elliptic equations, which are solved at each substep of the Runge-Kutta scheme. The regularised form of the evolution equations is used at the outermost grid point at $\mathscr{I}^+$.

As a first test problem, we consider a Schwarzschild black hole. The metric on constant mean curvature hypersurfaces was first derived in [6]. We evolved this spacetime for (at least) 10^3 times the mass of the black hole without any signs of instabilities. The difference between the numerical and the exact solution as well as the residual of the momentum constraints show approximate fourth-order convergence.
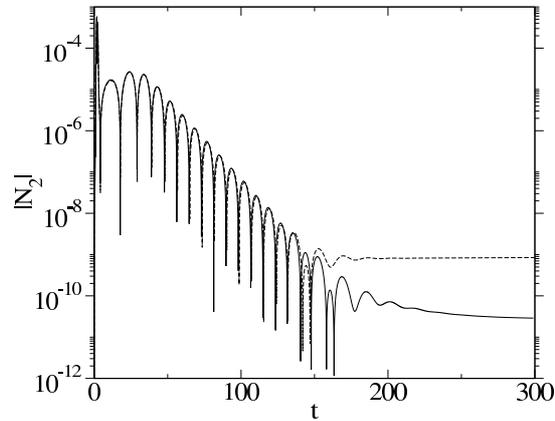
FIGURE 2. Quadrupole contribution ($\ell = 2$) to the Bondi news function at $\mathscr{I}^+$ for a perturbed Schwarzschild black hole (mass $M = 1$). Two different numerical resolutions are shown.

Next we include a gravitational wave perturbation. The Bondi news function [7], an invariant measure of gravitational radiation, is extracted at $\mathscr{I}^+$ (Fig. 2). The quasi-normal mode radiation emitted by the perturbed black hole is clearly visible. The frequency is in agreement with linear perturbation theory. (However we stress that the numerical simulation uses the full nonlinear Einstein equations.) Currently the numerical resolution is insufficient to resolve the power-law decay ('tail') expected at later times. The accuracy and efficiency of the numerical method needs to be improved; this will be the subject of future work.

REFERENCES

[1] R. Penrose, *Zero rest-mass fields including gravitation: asymptotic behaviour*, Proc. R. Soc. Lond. A **284** (1965), 159–203.

[2] H. Friedrich, *Cauchy problems for the conformal vacuum field equations in general relativity*, Commun. Math. Phys. **91** (1983), 445–72.

[3] L. Andersson, P. Chruściel and H. Friedrich, *On the regularity of solutions to the Yamabe equation and the existence of smooth hyperboloidal initial data for Einstein's field equations*, Commun. Math. Phys. **149** (1992), 587–612.

[4] V. Moncrief and O. Rinne, *Regularity of the Einstein equations at future null infinity*, Class. Quantum Grav. **26** (2009), 125010.

[5] O. Rinne, *An axisymmetric evolution code for the Einstein equations on hyperboloidal slices*, Class. Quantum Grav. **27** (2010), 035014.

[6] D. R. Brill, J. M. Cavallo and J. A. Isenberg, *K-surfaces in the Schwarzschild space-time and the construction of lattice cosmologies*, J. Math. Phys. **21** (1980), 2789–96.

[7] H. Bondi, M. G. J. van der Burg and A. W. K. Metzner, *Gravitational waves in general relativity VII. Waves from axi-symmetric isolated systems*, Proc. R. Soc. Lond. A **262** (1962), 21–52.

Geometric Evolution Equations related to Fluid Mechanics: On a Navier-Stokes/Mullins-Sekerka System

Helmut Abels

We consider the flow of two incompressible, viscous and (macroscopically) immiscible fluids inside a bounded, sufficiently smooth domain $\Omega \subset \mathbb{R}^n$, $n = 2, 3$, without contact angles. In classical sharp interface models the fluids, filling domains $\Omega^+(t)$ and $\Omega^-(t)$ for $t > 0$, are separated by a common interface $\Gamma(t)$ that is an $(n-1)$-dimensional surface. Surface tension effects are usually modeled with the aid of the Young-Laplace law

$$-\nu_{\Gamma(t)} \cdot [\![T(v,p)]\!] = \sigma H \nu_{\Gamma(t)} \qquad \text{on } \Gamma(t) \text{ for } t > 0,$$

where $[\![\ ]\!]$ denotes the jump of a quantity across the interface in direction of $\nu_{\Gamma(t)}$, i.e.,

$$[\![f]\!](x) = \lim_{h \to 0} (f(x + h\nu_{\Gamma(t)}) - f(x - h\nu_{\Gamma(t)})) \qquad \text{for } x \in \Gamma(t).$$

Here the flow is described in terms of the velocity $v \colon (0, \infty) \times \Omega \to \mathbb{R}^n$ and the pressure $p \colon (0, \infty) \times \Omega \to \mathbb{R}$ in both fluids in Eulerian coordinates. We assume the fluids to be of Newtonian type, i.e., the stress tensors of the fluids are of the form $T(v, p) = \mu^\pm Dv - pI$ in $\Omega^\pm(t)$ with constant viscosities $\mu^\pm > 0$ and $2Dv = \nabla v + \nabla v^T$. Furthermore, we denote by $\nu_{\Gamma(t)}$ the unit normal of $\Gamma(t)$ that points outside $\Omega^+(t)$, by V and H the normal velocity and scalar mean curvature of $\Gamma(t)$ with respect to $\nu_{\Gamma(t)}$, and σ is a constant surface tension coefficient.

In classical models (without phase transitions) the interface $\Gamma(t)$ is usually material, i.e., it is transported by the bulk velocities:

$$V = \nu_{\Gamma(t)} \cdot v|_{\Gamma(t)} \quad \text{on } \Gamma(t) \text{ for } t > 0.$$

But in some situations diffusional effects play a role and the interface is no longer material. E.g. in certain polymer mixtures spinodal decomposition can occur, which is diffusion driven, cf. [10]. The following non-classical model is capable to describe such situations.

The considered model leads to the following system of Navier-Stokes/Mullins-Sekerka type:

$$
\begin{array}{lll}
(1) & \partial_t v + v \cdot \nabla v - \operatorname{div} T(v, p) = 0 & \text{in } \Omega^\pm(t) \text{ for } t > 0, \\
(2) & \operatorname{div} v = 0 & \text{in } \Omega^\pm(t) \text{ for } t > 0, \\
(3) & m\Delta\mu = 0 & \text{in } \Omega^\pm(t) \text{ for } t > 0, \\
(4) & -\nu_{\Gamma(t)} \cdot [\![T(v,p)]\!] = \sigma H \nu_{\Gamma(t)} & \text{on } \Gamma(t) \text{ for } t > 0, \\
(5) & V - \nu_{\Gamma(t)} \cdot v|_{\Gamma(t)} = -m[\![\nu_{\Gamma(t)} \cdot \nabla\mu]\!] & \text{on } \Gamma(t) \text{ for } t > 0, \\
(6) & \mu|_{\Gamma(t)} = \sigma H & \text{on } \Gamma(t) \text{ for } t > 0.
\end{array}
$$

We close the system by adding the initial and boundary conditions

(7) $$v|_{\partial\Omega} = 0 \qquad \text{on } \partial\Omega \text{ for } t > 0,$$

(8) $$\nu_\Omega \cdot m\nabla\mu|_{\partial\Omega} = 0 \qquad \text{on } \partial\Omega \text{ for } t > 0,$$

(9) $$\Omega^+(0) = \Omega_0^+,$$

(10) $$v|_{t=0} = v_0 \qquad \text{in } \Omega,$$

where v_0, Ω_0^+ are given initial data satisfying $\partial\Omega_0^+ \cap \partial\Omega = \emptyset$ and where $m > 0$ is a mobility constant. Here it is assumed that v and μ do not jump across $\Gamma(t)$, i.e.,

$$[\![v]\!] = [\![\mu]\!] = 0 \qquad \text{on } \Gamma(t) \text{ for } t > 0.$$

Equations (1)-(2) describe the conservation of linear momentum and mass in both fluids and (4) is the balance of forces at the boundary. The equations for v are complemented by the non-slip condition (7) at the boundary of Ω. The conditions (3), (8) describe together with (5) a continuity equation for the masses of the phases, and (6) relates the chemical potential μ to the L_2-gradient of the surface area, which is given by the mean curvature of the interface. Here the densities of the fluids are assumed to be the same and for simplicity set to one.

We note that (1)-(10) appears as a sharp interface limit of the following diffuse interface model, introduced by Hohenberg and Halperin [7] and rigorously derived by Gurtin et al. [6]:

(11) $$\partial_t v + v \cdot \nabla v - \operatorname{div}(\nu(c)Dv) + \nabla p = -\varepsilon \operatorname{div}(\nabla c \otimes \nabla c) \qquad \text{in } \Omega \times (0, \infty),$$

(12) $$\operatorname{div} v = 0 \qquad \text{in } \Omega \times (0, \infty),$$

(13) $$\partial_t c + v \cdot \nabla c = m\Delta\mu \qquad \text{in } \Omega \times (0, \infty),$$

(14) $$\mu = \varepsilon^{-1} f'(c) - \varepsilon\Delta c \qquad \text{in } \Omega \times (0, \infty),$$

(15) $$v|_{\partial\Omega} = 0 \qquad \text{on } \partial\Omega \times (0, \infty),$$

(16) $$\partial_n c|_{\partial\Omega} = \partial_n \mu|_{\partial\Omega} = 0 \qquad \text{on } \partial\Omega \times (0, \infty),$$

(17) $$(v, c)|_{t=0} = (v_0, c_0) \qquad \text{in } \Omega.$$

Here c is the concentration of one of the fluids, where we note that a partial mixing of both fluids is assumed in the model, and f is a suitable "double-well potential" e.g. $f(c) = c^2(1-c)^2$. Moreover, $\varepsilon > 0$ is a small parameter related to the interface thickness, μ is the so-called chemical potential and $m > 0$ is the mobility. We refer to [1, 4] for some analytic results. For some results on the sharp interface limit of (11)-(17) we refer to A. and Röger [3, Appendix] and A., Garcke, and Grün [2]. Existence of weak solutions of (1)-(10) was proved in [3].

In a joint-work with Mathias Wilke we prove existence of strong solutions of (1)-(10) locally in time. To this end we first prove existence of a unique strong solutions of the Navier-Stoke system (1), (2), (4), (7), (10) for a given interface $\Gamma(t)$ and sufficiently small times. This is done with the aid of a coordinate transformation to the initial domains $\Omega_0^\pm$ and an application of a contraction argument using maximal regularity of the linearized system in L^2-Sobolev spaces for v of second order in space and first order in time. Then the coupled system is solved by using

the so-called Hanzawa transformation to transform the Mullins-Sekerka part (3), (5), (6), (8), (9) to an evolution equation for a height function $h\colon \Sigma \times (0,T) \to \mathbb{R}$. The coupling to the Navier-Stokes systems yields a new term, which is non-local in space and time, but of lower order. Therefore for small times the principal part of the Mullins-Sekerka equation dominates this term and existence of strong solutions is proved in a similar manner as in the case of a single Mullins-Sekerka equation, cf. Escher and Simonett [5] or Köhne et al. [8]. We note that we construct the height function h in the space $L^p(0,T;W_p^{4-\frac{1}{p}}(\Sigma)) \cap W_p^1(0,T;W_p^{1-\frac{1}{p}}(\Sigma))$ for a suitable $p > 3$, while the velocity v is in an L^2-Sobolev space. Since the coupling to the Navier-Stokes system is of lower order, an L^2-theory is sufficient for the Navier-Stokes part. Finally, we show stability of equilibria, which consist of a vanishing velocity and spherical interfaces. This is done by adopting the arguments of the proof the generalized principle of linearized stability of Prüss et al. [9] to the present situation.

References

[1] H. Abels. On a diffuse interface model for two-phase flows of viscous, incompressible fluids with matched densities. *Arch. Rat. Mech. Anal.*, 194(2):463–506, 2009.

[2] H. Abels, H. Garcke, and G. Grün. Thermodynamically consistent, frame indifferent diffuse interface models for incompressible two-phase flows with different densities. *Preprint, arXiv:/1104.1336, to appear in "Math. Models Methods Appl. Sci."*, 2011.

[3] H. Abels and M. Röger. Existence of weak solutions for a non-classical sharp interface model for a two-phase flow of viscous, incompressible fluids. *Ann. Inst. H. Poincaré Anal. Non Linéaire*, 26:2403–2424, 2009.

[4] F. Boyer. Mathematical study of multi-phase flow under shear through order parameter formulation. *Asymptot. Anal.*, 20(2):175–212, 1999.

[5] J. Escher and G. Simonett. A center manifold analysis for the Mullins-Sekerka model. *J. Differential Equations*, 143(2):267–292, 1998.

[6] M. E. Gurtin, D. Polignone, and J. Viñals. Two-phase binary fluids and immiscible fluids described by an order parameter. *Math. Models Methods Appl. Sci.*, 6(6):815–831, 1996.

[7] P.C. Hohenberg and B.I. Halperin. Theory of dynamic critical phenomena. *Rev. Mod. Phys.*, 49:435–479, 1977.

[8] M. Köhne, J. Prüss, and M. Wilke. On quasilinear parabolic evolution equations in weighted L_p-spaces. *J. Evol. Equ.*, 10(2):443–463, 2010.

[9] J. Prüss, G. Simonett, and R. Zacher. On convergence of solutions to equilibria for quasilinear parabolic problems. *J. Differential Equations*, 246(10):3902–3931, 2009.

[10] I. Roušar and E.B. Naumann. Spinodal decomposition with surface tension driven flows. *Chemical Engineering Communications*, 105(1):77–98, 2010.

Geometric pdes, finite element exterior calculus, adaptive methods, and applications in relativity

Michael Holst

We examine the theory and numerical treatment of coupled nonlinear elliptic geometric PDE containing critical exponents. A motivating example is the conformal formulation of the Einstein equations. We first outline some new results for existence of solutions to the constrained equations for rough metrics and arbitrarily

prescribed mean extrinsic curvature. We then develop some new a priori error estimates for Galerkin finite element approximation; the estimates have the surprising feature that no angle conditions are involved in the case of critical and subcritical nonlinearity. Moreover, it then becomes possible to turn the a priori estimates into pointwise control of the discrete solutions, without the need for a discrete maximum principle, and hence again without the need for angle conditions. We then describe a new approach to analyzing the geometric error made if the domain is a smooth Riemannian manifold rather than a polyhedral domain. The approach involves the development of variational crimes analysis in Hilbert complexes, and we subsequently use this abstract framework to develop analogues of the Strang Lemmas for the finite element exterior calculus (FEEC). We show how new variational crimes framework in FEEC completely recovers the classical a priori surface finite element estimates of Dziuk and Demlow, and further generalizes their results to hypersurfaces of arbitrary spatial dimension, to the Hodge Laplacian, and to nonlinear problems involving arbitrary order differential forms.

Discrete geodesic calculus in shape space
MARTIN RUMPF
(joint work with Benedikt Wirth)

We develop a time discrete calculus on the infinite dimensional Riemannian manifold of volumetric objects with a metric which reflects the viscous dissipation caused by a deformation of the fluid like objects. The approach is based on a local approximation of the squared Riemannian distance by a computationally cheap energy functional, whose Hessian reproduces the underlying Riemannian metric. This is used to define length and energy of discrete paths in shape space. The notion of discrete geodesics defined as energy minimizing paths gives rise to a discrete logarithmic map, a variational definition of a discrete exponential map, and a time discrete parallel transport. Applications are shown for topology preserving shape morphing, the representation of paths in shape space via local shape variations as path generators, shape extrapolation via discrete geodesic flow, and the transfer of geometric features.

Shape space as a Riemannian manifold. Geodesic paths in shape space allow to define smooth and in some sense geometrically or physically natural connecting paths $\mathcal{O}(t)$, $t \in [0, 1]$, between two given shapes $\mathcal{O}(0), \mathcal{O}(1)$, or they enable the extrapolation of a path from an initial shape $\mathcal{O}(0)$ and an initial shape variation $\delta\mathcal{O}$ which encodes the path direction. As locally length minimizing paths, geodesic paths require to endow the space of shapes with a Riemannian metric which encodes the preferred shape variations. There is a rich diversity of Riemannian shape spaces in the literature. Kilian et al compute isometry invariant geodesics between consistently triangulated surfaces [5], where the Riemannian metric measures stretching of triangle edges. A morphing approach based on the concept

of optimal mass transport has been proposed by Haker et al [3, 7]. Dupuis et al employ a metric $\mathcal{G}(v, v) = \int_D Lv \cdot v \, dx$ with a higher order elliptic operator L on some computational domain D [1] ensuring a diffeomorphism property of geodesic paths. Fuchs et al propose a viscous-fluid based Riemannian metric [2]. Preliminary results on the time discrete geodesic calculus have been presented by Wirth et al [6].

The space of viscous-fluid objects. Let us introduce the space $\mathcal{M}$ of shapes as the set of volumetric objects $\mathcal{O}$. A smooth path $(\mathcal{O}(t))_{t \in [0,1]}$ in this shape space is associated with a smooth family $(\phi(t))_{t \in [0,1]}$ of deformations. To measure the distance between two objects a Riemannian metric

$$\mathcal{G}_{\mathcal{O}}(v, v) = \min_{\{\tilde{v} \,|\, \tilde{v} \cdot n = v \cdot n \text{ on } \partial\mathcal{O}\}} \int_{\mathcal{O}} \mathbf{diss}(\nabla \tilde{v}(x)) \, dx \,.$$

is defined on velocity fields v on $\partial\mathcal{O}$, where $\mathbf{diss}(\nabla v) = \lambda(\mathrm{tr}\epsilon[v])^2 + 2\mu\mathrm{tr}(\epsilon[v]^2)$ for $\epsilon[v] := \frac{1}{2}(\nabla v + \nabla v^T)$ reflects the internal fluid friction—called dissipation—that occurs while the object is deformed. Then, the path energy E is defined as

$$\mathrm{E}[(\mathcal{O}(t))_{t \in [0,1]}] = \int_0^1 \mathcal{G}_{\mathcal{O}(t)}(v(t), v(t)) \, dt \,.$$

Paths which (locally) minimize the energy E are geodesics. A geodesic thus mimics the energetically optimal way to continuously deform a fluid volume into a different volume.

Approximating the distance and discrete geodesics. We use an efficient and robust time discrete approximation based on an polyconvex energy functional $\mathcal{W}$ which locally behaves like the squared Riemannian distance with

$$\mathrm{dist}^2(\mathcal{O}, \tilde{\mathcal{O}}) = \min_{\psi(\mathcal{O}) = \tilde{\mathcal{O}}} \mathcal{W}_{\mathcal{O}}[\psi] + O(\mathrm{dist}^3(\mathcal{O}, \tilde{\mathcal{O}})) \,.$$

Given this approximation, we are in a position to define a discrete path energy

$$\mathrm{E}[(\mathcal{O}_0, \ldots, \mathcal{O}_K)] = \frac{1}{\tau} \sum_{k=1}^K \mathcal{W}_{\mathcal{O}_{k-1}}[\psi_k] \,,$$

on a discrete path $(\mathcal{O}_0, \ldots, \mathcal{O}_K)$ where $\mathcal{O}_k \approx \mathcal{O}(t_k)$ with $t_k = k\tau$ for $k = 0, \ldots, K$ ($\tau = \frac{1}{K}$). Here, $\psi_k = \mathrm{argmin}_{\psi(\mathcal{O}_{k-1}) = \mathcal{O}_k} \mathcal{W}_{\mathcal{O}_{k-1}}[\psi]$. A *discrete geodesic* (of order K) is now defined as a minimizer of $\mathrm{E}[(\mathcal{O}_0, \ldots, \mathcal{O}_K)]$ for fixed end points $\mathcal{O}_0, \mathcal{O}_K$.

Discrete logarithm and discrete exponential map. Let $(\mathcal{O}_0, \ldots, \mathcal{O}_K)$ be a discrete geodesic between $\mathcal{O} = \mathcal{O}_0$ and $\tilde{\mathcal{O}} = \mathcal{O}_K$ with an associated sequence of optimal matching deformations $\psi_1, \ldots, \psi_K$, then we define the discrete $\frac{1}{K}$ logarithm as

$$(\tfrac{1}{K}\mathrm{LOG})_{\mathcal{O}}(\tilde{\mathcal{O}}) := \zeta_1$$

for the displacement $\zeta_1(x) = \psi_1(x) - x$. Furthermore, we define the discrete power k exponential map EXP^k as an approximation of $\exp(k\cdot)$ via

$$\mathrm{EXP}^1_{\mathcal{O}}(\zeta) := (\tfrac{1}{1}\mathrm{LOG})^{-1}_{\mathcal{O}}(\zeta),$$

$$\mathrm{EXP}^2_{\mathcal{O}}(\zeta) := (\tfrac{1}{2}\mathrm{LOG})^{-1}_{\mathcal{O}}(\zeta),$$

$$\mathrm{EXP}^k_{\mathcal{O}}(\zeta) := \mathrm{EXP}^2_{\mathcal{O}_{k-2}}(\zeta_{k-1})$$

$$\text{with } \zeta_{k-1} := (\tfrac{1}{1}\mathrm{LOG})_{\mathrm{EXP}^{k-2}_{\mathcal{O}}(\zeta)}\mathrm{EXP}^{k-1}_{\mathcal{O}}(\zeta).$$

Experimentally we observe the following convergence behaviour

$$k(\tfrac{1}{k}\mathrm{LOG})_{\mathcal{O}}(\tilde{\mathcal{O}}) \to \log_{\mathcal{O}}(\tilde{\mathcal{O}})$$

$$\mathrm{EXP}^k_{\mathcal{O}}\left(\tfrac{1}{k}\zeta\right) \to \exp_{\mathcal{O}}(\zeta)$$

for $k \to \infty$.

Discrete parallel transport. There is a well-known first-order approximation of parallel transport called Schild's ladder [4], which is based on the construction of a sequence of geodesic parallelograms where the two diagonal geodesics always meet at their midpoints. Using the above defined discrete logarithm and discrete exponential map, we obtain the following scheme to compute the time discrete parallel transport of a displacement ζ_{k-1} along the edge from $\mathcal{O}_{k-1}$ to $\mathcal{O}_k$

$$\mathcal{O}^p_{k-1} = \mathrm{EXP}^1_{\mathcal{O}_{k-1}}\zeta_{k-1},$$

$$\mathcal{O}^\times_k = \mathrm{EXP}^1_{\mathcal{O}^p_{k-1}}\left((\tfrac{1}{2}\mathrm{LOG})_{\mathcal{O}^p_{k-1}}(\mathcal{O}_k)\right),$$

$$\mathcal{O}^p_k = \mathrm{EXP}^2_{\mathcal{O}_{k-1}}\left((\tfrac{1}{1}\mathrm{LOG})_{\mathcal{O}_{k-1}}(\mathcal{O}^\times_k)\right),$$

$$\zeta_k = (\tfrac{1}{1}\mathrm{LOG})_{\mathcal{O}_k}(\mathcal{O}^p_k),$$

where ζ_k is the transported displacement on $\mathcal{O}_k$. Here, $\mathcal{O}^\times_k$ is the midpoint of the two geodesics with end points $\mathcal{O}^p_{k-1}$, $\mathcal{O}_k$ and $\mathcal{O}_{k-1}$, $\mathcal{O}^p_k$, respectively.

Remark: As in the continuous case, the discrete parallel transport can be used to define a discrete Levi-Civita connection.

REFERENCES

[1] D. Dupuis, U. Grenander, and M. Miller. Variational problems on flows of diffeomorphisms for image matching. *Quarterly of Applied Mathematics*, 56:587–600, 1998.

[2] M. Fuchs, B. Jüttler, O. Scherzer, and H. Yang. Shape metrics based on elastic deformations. *J. Math. Imaging Vis.*, 35(1):86–102, 2009.

[3] S. Haker, A. Tannenbaum, and R. Kikinis. Mass preserving mappings and image registration. *Proceedings of Fourth International Conference on Medical Image Computing and Computer-Assisted Intervention*, pages 120–127, 2001.

[4] A. Kheyfets, W. A. Miller, and G. A. Newton. Schild's ladder parallel transport procedure for an arbitrary connection. *Internat. J. Theoret. Phys.*, 39(12):2891–2898, 2000.

[5] M. Kilian, N. J. Mitra, and H. Pottmann. Geometric modeling in shape space. In *ACM Transactions on Graphics*, volume 26, pages #64, 1–8, 2007.

[6] B. Wirth, L. Bar, M. Rumpf, and G. Sapiro. A continuum mechanical approach to geodesics in shape space. *IJCV*, 93(3):293–318, 2011.

[7] L. Zhu, Y. Yang, S. Haker, and A. Tannenbaum. An image morphing technique based on optimal mass preserving mapping. *IEEE Transactions on Image Processing*, 16(6):1481–1495, 2007.

Mean curvature evolution of hypersurfaces
Klaus Ecker

In this talk, we reviewed joint results with Gerhard Huisken ([1], [2]) on the mean curvature evolution of hypersurfaces of entire graphs, that is solutions $u(\cdot, t)$ of the Cauchy problem

$$\frac{\partial u}{\partial t} = \sqrt{1 + |Du|^2} \operatorname{div}\left(\frac{Du}{\sqrt{1 + |Du|^2}}\right)$$

on $\mathbb{R}^n \times (0, T)$, $u(\cdot, 0) = u_0$ on $\mathbb{R}^n$, where $T \in (0, \infty]$.

It turns out that, in contrast to the analogous problem for the standard heat equation, there always exists a smooth solution for all positive times as long as u_0 is locally Lipschitz (for instance $u_0 \in C^1(\mathbb{R}^n)$ is sufficient). In particular, no growth assumption on u_0 or a prescription of the growth class of the solution is necessary, see [2].

Some of the techniques include maximum principle arguments of the following form: If M_t denotes the evolving hypersurface and ∇^{M_t} and Δ_{M_t} its tangential gradient and Laplace-Beltrami operator respectively, and if we consider a function f on M_t (which is allowed to depend on time explicitly) which is smooth for $t \in (0, T]$ and continuous up to $t = 0$ and which satisfies an inequality of the form

$$(1) \qquad \left(\frac{d}{dt} - \Delta_{M_t}\right) f \leq a \cdot \nabla^{M_t} f$$

for all $t \in (0, T]$ for some vectorfield a on M_t (here d/dt denotes the total time derivative) then in many situations we may conclude that

$$(2) \qquad \sup_{M_t} f \leq \sup_{M_0} f$$

for all times $t \in [0, T]$ for which the vectorfield a is well-defined.

For compact solutions of mean curvature flow, the maximum principle follows from an easy calculus argument, but using more involved methods it can also be shown to hold on non-compact solutions such as solutions of our above Cauchy problem if the latter satisfy certain additional conditions, see [1], [2]. If such conditions are not satisfied one can instead employ a localized version of the maximum principle, but for this to work the function f above would have to satisfy a more restrictive inequality than (1). These conditions, however, can be shown to hold for interesting functions f from which the necessary geometric information about our solution can be gleaned, see [2].

Here are some examples of useful geometric functions f satisfying (1) taken from [1]: Let ν denote the upper normal to our evolving graphs and consider the function

$$v = \frac{1}{\nu \cdot e_{n+1}}$$

(e_{n+1} is the unit vector in $\mathbb{R}^n$ with respect to which the solution is written as a graph. Th e quantity v is well-defined as long as the solution is graphical. Moreover, up to tangential diffeomorphisms, it agrees with the expression $\sqrt{1 + |Du|^2}$. It also satisfies the inequality $v \geq 1$ which will be used in a little while. A bound on v would yield a gradient bound for our solution. A direct geometric calculation using the non-graphical version of the equation for mean curvature flow given by

$$\frac{\partial x}{\partial t} = -H\nu,$$

where H denotes the mean curvature of the evolving hypersurfaces M_t, implies that $f = v$ satisfies (1) with $a = 0$. Therefore we conclude from (2) that

$$\sup_{M_t} v \leq \sup_{M_0} v$$

for all $t \in [0, T]$, that is if initially the gradient is bounded it is bounded at later times by the same constant. This estimate is one of the key steps in establishing longtime existence of a solution for he above Cauchy problem, at least in the case of linearly growing initial data.

A more complicated function is given by $f = 2t|A|^2 v^2 + v^2$ where $|A|^2$ denotes the squared norm of the second fundamental form of the solution (which in the presence of a gradient bound is comparable to the square of the Hessian of u). A more involved calculation combined with some analytic estimation tricks shows that also this f satisfies (1), in this case with

$$a = -\frac{2}{v} \nabla^{M_t} v$$

which is bounded by $2|A|v$. If we now again assume that $\sup_{M_0} v \leq c_0 < \infty$, inequality (2) implies that

$$\sup_{M_t} \left(2t|A|^2 v^2 + v^2 \right) \leq c_0^2$$

for all $t \geq 0$ from which we conclude that $|A|^2$ has to decay to zero for time to infinity if we already know that the solution exists for all time.

Note that the maximum principle is applicable to this partiular f despite the dependence of a on f. We are more or less saying that if f is not already infinitely large than it is controlled by its initial supremum which then in turn implies that it can never become infinitely large.

REFERENCES

[1] K. Ecker and G. Huisken, Mean curvature evolution of entire graphs, Annals of Math **130**, 453 - 471 (1989)
[2] K. Ecker and G. Huisken, Interior estimates for hypersurfaces moving by mean curvature, Invent. math. **105**, 547 - 569 (1991)

CubeCover - Cubical grids for bounded volumes

KONRAD POLTHIER

(joint work with Matthias Nieser, Ulrich Reitebuch)

We discuss novel techniques to fill a bounded volumetric shape with a (preferably coarse) cubical voxel structure. Among the optimization goals are alignment of the voxels with the bounding surface as well as simplicity of the voxel grid. Mathematical analysis of the possible singularities is given.

The algorithm is uses a tetrahedral volume mesh plus a user given guiding frame field as input. Then it constructs an atlas of chart functions, i.e. the parameterization function of the volume, such that the images of the coordinate lines align with the given frame field. Formally the function is given by a first-order PDE, namely the gradients of the coordinate functions are the vectors of the frame. In a first step, the algorithm uses a discrete Hodge decomposition to assure local integrability of the frame field. A subsequent step assures global integrability along generators of the first homology group and alignment a face of the boundary cube with the original surface boundary. All steps can be merged into solving linear equations.

The figure below shows a cubified CAD model (rockerarm) obtained from an original tetrahedral volume mesh. Conceptually the presented CubeCover-algorithm extends the known QuadCover-algorithm from surface meshes to volumes meshes.
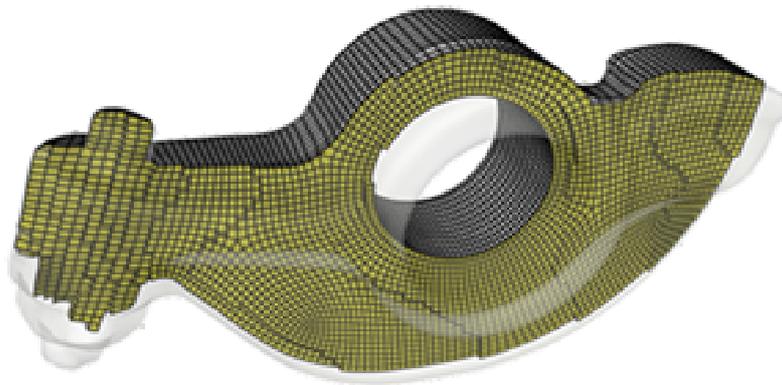
References

[1] M. Nieser, U. Reitebuch, K. Polthier, *CubeCover - Parameterization of 3D Volumes*, Computer Graphics Forum **30** (2011), 1397–1406.

Geodesic Finite Elements

Oliver Sander

We consider partial differential equations for functions

$$f : \Omega \to M,$$

where Ω is an open subset of $\mathbb{R}^d$, and M a nonlinear Riemannian manifold. Such problems cannot be discretized using finite elements, because the standard definition of finite element functions presupposes a vector space structure on M. Instances of such problems are, for example, the simulation of liquid crystals [2] (with $M = S^2$, $\mathbb{RP}^2$, or SO(3)), or the numerical treatment of Cosserat materials [5] (with $M = \mathbb{R}^3 \times$ SO(3)).

Various ways have been proposed in the literature to discretize problems for functions with values in a manifold M. We would like to mention the approach of Bartels and Prohl [1], who used an embedding of M in a Euclidean space $\mathbb{R}^m$. The values are interpolated in $\mathbb{R}^m$, and only vertex values are constrained to be on M. While this is simple, and in many cases cheap and even objective, the result depends on the embedding.

In [6] we have introduced geodesic finite elements as a conforming finite element discretization for partial differential equations for functions with values in a Riemannian manifold M. In the present contribution we explain the idea and then generalize it to obtain finite elements of higher order. This paves the way for advanced discretization methods like *hp*- and *DG*-methods, and for hierarchical error estimators.

Let Δ be the d-dimensional reference simplex, with coordinates ξ and barycentric coordinates $w = w(\xi)$. In [6], the following generalization of linear interpolation was introduced.

Definition 1. *Let M be a connected Riemannian manifold and* $\mathrm{dist}(\cdot, \cdot) : M \times M \to \mathbb{R}$ *a distance metric on M. For a set of values $v = (v_1, \dots, v_{d+1}) \in M^{d+1}$ at the simplex corners we call*

$$\Upsilon \ : \ M^{d+1} \times \Delta \to M$$

$$\text{(1)} \qquad \Upsilon(v, \xi) = \underset{q \in M}{\arg\min} \sum_{i=1}^{d+1} w_i(\xi) \, \mathrm{dist}(v_i, q)^2$$

geodesic interpolation on M.

This definition is motivated by the corresponding formula for linear spaces. Indeed, if $M = \mathbb{R}$, then (1) reduces to linear interpolation.

Unlike for linear spaces, it is not clear, however, whether (1) always has a unique solution. Existence and uniqueness of a minimizer can be obtained if the values $v_1, \ldots, v_{d+1}$ are "close together" in a certain sense. The precise conditions have been given by Karcher [4].

Theorem 1 (Karcher [4]). *Let M be complete, B_ρ an open geodesic ball of radius ρ in M, and $v_1, \ldots, v_{d+1} \in M$. Assume that $v_i \in B_\rho$ for all $i = 1, \ldots, d+1$.*

(1) *If the sectional curvatures of M in B_ρ are bounded by a positive constant K, and $\rho < \frac{1}{4}\pi K^{-1/2}$, then the function*

$$f_{v,w}(q) := \sum_{i=1}^{d+1} w_i \operatorname{dist}(v_i, q)^2$$

has a unique minimizer in B_ρ for all $w \in \Delta$.

(2) *If the sectional curvatures of M in B_ρ are at most 0, then $f_{v,w}$ has a unique minimizer in B_ρ for all $w \in \Delta$.*

The requirement for the v_i to be "close together" for Υ to be well-defined is not a serious restriction in a finite element context. There, many properties are expected to hold on sufficiently fine grids only, anyways. In [6] it is shown that the conditions of Theorem 1 are fulfilled if the grid is fine enough.

The interpolation procedure given by Definition 1 has various desirable properties. In particular, it is infinitely differentiable with respect to ξ and the v_i, [6, Thm. 2.2], and equivariant under isometries of M, [6, Lem. 2.6]. It can therefore be used to construct finite element functions for simplicial grids G of Ω. The resulting discretizations are conforming in the sense that such finite element functions are elements of the Sobolev space $H^1(\Omega, M)$.

To obtain generalizations for higher-order interpolation formulas, let $\{\varphi_i^p, i = 1, \ldots, m\}$ be the p-th-order Lagrangian shape functions on Δ, and let v_i, $i = 1, \ldots, m$ be values at the Lagrange nodes. In a linear space p-th order interpolation is then given by $\Upsilon^p(v, \xi) = \sum_{i=1}^m \varphi_i^p(\xi) v_i$. To generalize this to functions with values in a Riemannian manifold M we try to write it as a minimization problem. This is surprisingly easy; we obtain the following definition, which, incidentally, also works for non-simplex reference elements.[1]

Definition 2. *Let M be a connected Riemannian manifold and $\operatorname{dist}(\cdot, \cdot) : M \times M \to \mathbb{R}$ a distance metric on M. Let $\{\varphi_i^p, i = 1, \ldots, m\}$ be a set of p-th order scalar Lagrangian shape functions, and let $v_i \in M$, $i = 1, \ldots, m$ be values at the corresponding Lagrange nodes. We call*

$$\Upsilon^p \ : \ M^m \times \Delta \to M$$

$$\Upsilon^p(v_1, \ldots, v_m; \xi) = \arg\min_{q \in M} \sum_{i=1}^m \varphi_i^p(\xi) \operatorname{dist}(v_i, q)^2$$

---

[1]Recently we learned of the work of Philipp Grohs [3], who independently came up with the same approach to higher-order interpolation in nonlinear spaces.

p-th order geodesic interpolation on M.

Obviously, this construction produces an interpolation function of the values v_i. Also, it comprises the previous Definition 1 for the first-order case, because we have $w_i(\xi) = \varphi_i^1(\xi)$ for all $\xi \in \Delta$ and $i = 1, \ldots, 3$.

The well-posedness again needs consideration. Karcher's proof of Theorem 1 does not cover Definition 2, because the interpolation weights φ_i^p can be negative. It is nevertheless conjectured that a weaker form of the theorem does hold.

On the other hand, further properties like differentiability of Υ^p, and its equivariance under isometries of M can be proved just like in the first-order case. The higher-order interpolation formula can therefore be used as the basis of a theory of conforming finite elements. First numerical tests show that optimal discretization error behavior can be obtained.

<div align="center">REFERENCES</div>

[1] S. Bartels and A. Prohl, *Constraint preserving implicit finite element discretization of harmonic map flow into spheres*, Math. Comp. **76** 260 (2007), 1847–1859.
[2] P.G. de Gennes and J. Prost, *The Physics of Liquid Crystals*, Clarendon Press (1993)
[3] P. Grohs, *Finite elements of arbitrary order and quasiinterpolation for Riemannian data*, SAM Report, ETH Zürich **2011-56** (2011)
[4] H. Karcher, *Riemannian center of mass and mollifier smoothing*, Comm. Pure Appl. Math. **30** (1977), 509–541.
[5] P. Neff, *Geometrically exact Cosserat theory for bulk behavior and thin structures. Modeling and mathematical analysis*, Habilitationsschrift, Technische Universität Darmstadt (2003)
[6] O. Sander, *Geodesic finite elements on simplicial grids*, submitted

<div align="center">

Conservation laws on moving surfaces

DIETMAR KRÖNER

(joint work with Gerd Dziuk, Thomas Müller)

</div>

Several phenomena like relativistic flows, transport processes on surfaces, transport of oil on the waves of the ocean or the transport of species on moving interfaces between two fluid are modeled by transport equations on fixed or moving surfaces. Here we consider the following situation.

Assumptions 0.1. *Let $\Gamma_t = \Gamma(t) \subset \mathbb{R}^{n+1}$ for $t \in [0, T]$ be a time dependent, compact, closed, smooth hypersurface. The initial surface Γ_0 is transported by the smooth function $\Phi : \Gamma_0 \times [0, T] \to \mathbb{R}^{n+1}$ with $\Phi(\Gamma_0, t) = \Gamma_t$ and $\Phi(\cdot, 0) = Id$. We assume that $\Phi(\cdot, t) : \Gamma_0 \to \Gamma(t)$ is a diffeomorphism for every $t \in [0, T]$. The velocity of the material points is denoted by $v := \partial_t \Phi \circ \Phi^{-1}$. Let $f = f(x, t, u)$ be a flux function which is a family of vector fields such that $f(x, t, u)$ is a tangent vector to the surface Γ_t for $x \in \Gamma_t$, $t \in [0, T]$ and $u \in \mathbb{R}$. We assume that $\nabla_\Gamma \cdot f(., t, s) = 0$ for all fixed $t \in \mathbb{R}^+$, $s \in \mathbb{R}$. The definition of $\nabla_\Gamma \cdot$ is given below.*

Now we consider the following initial value problem for $u(\cdot, t) : \Gamma_t \to \mathbb{R}$.

(1) $\qquad \dot{u} + u\nabla_\Gamma \cdot v + \nabla_\Gamma \cdot f(.,u) \;=\; 0 \quad \text{on } G_T := \cup_t \Gamma(t) \times \{t\}$

(2) $\qquad\qquad\qquad\qquad\qquad u \;=\; u_0 \text{ on } \Gamma_0 \times \{0\}.$

The derivatives $\dot{g}$ and $\nabla_\Gamma g$ are defined as follows.

$$\nabla_\Gamma g = \nabla g - \nabla g \cdot \nu\, \nu \quad \text{on} \quad \Gamma_t, \quad \dot{g} = \frac{\partial g}{\partial t} + v \cdot \nabla g \quad \text{on} \quad G_T,$$

where ν is the normal to Γ_t. The aim of this contribution is to present the ideas of the proof for existence and uniqueness of an entropy solution of (1), (2), to develop a numerical scheme and to show some numerical experiments.

Let us briefly summarize the published results related to this topic. Total variation estimates for finite volume schemes on time independent Riemannian manifolds can be found in [1], [6], an existence proof of entropy solutions on time independent Riemannian manifolds is shown in [2], a finite volume scheme for conservation laws on a time independent Riemannian manifold including error estimates is presented in [8]. A wave propagation algorithm for hyperbolic systems on manifolds with applications in relativistic hydrodynamics and magnetohydrodynamics has been developed in [10], and finite volume schemes on spherical domains, partially with adaptive grid refinement in [3]. Finite element schemes for diffusion problems on moving surfaces has been studied in [5] and finite volume schemes in [9].

As in the Euclidean case classical solutions of (1), (2) do not exist globally in time. Therefore we have to define (weak) entropy solutions.

Lemma 0.2. *(entropy condition) Let $f =: (f_1, \cdots, f_{n+1})$, $q := (q_1, \cdots, q_{n+1})$, $\eta \in C^2(\mathbb{R})$, $\eta'' \geq 0$, $q_l(\cdot, s) := \int_{s_0}^s \eta'(\tau) f_l'(\cdot, \tau) d\tau$ for $l = 1, \cdots, n+1$ and $u_{0\varepsilon} \in L^\infty(\Gamma_0)$. Let u_ε be the smooth solution of*

$$\dot{u}_\varepsilon + u_\varepsilon \nabla_\Gamma \cdot v + \nabla_\Gamma \cdot f(.,u_\varepsilon) - \varepsilon \Delta_\Gamma u_\varepsilon \;=\; 0 \quad \text{on } G_T$$

(3) $\qquad\qquad\qquad\qquad\qquad u_\varepsilon \;=\; u_{0\varepsilon} \text{ on } \Gamma_0 \times \{0\}.$

and assume that $u_\varepsilon \to u$ a.e. on G_T, $u_{0\varepsilon} \to u_0$ on Γ_0 and $u \in L^1(G_T)$. Then u satisfies

(4) $\quad -\displaystyle\int_{\Gamma_0} \eta(u_0)\phi(\cdot,0) + \int_0^T \int_{\Gamma_t} \big[-\eta(u)\dot{\phi}(\cdot,t) - q(\cdot,u)\nabla_\Gamma\phi + \phi\nabla_\Gamma \cdot v(u\eta'(u) - \eta(u)) \big] \leq 0$

for all test functions $\phi \in H^1(G_T)$, $\phi \geq 0$ and $\phi(\cdot,T) = 0$ and all η and q with the properties, mentioned above.

Now we use (4) to define an entropy solution.

Definition 0.3. *(entropy solution) Let η, q_l and u_0 be as in Lemma 0.2. Then $u(\cdot,t) \in L^\infty(\Gamma_t) \cap L^\infty(\Gamma_t)$ is an entropy solution (or an admissible weak solution) of (1), (2) if u satisfies (4).*

In order to solve the conservation law (1), (2) we have to solve the initial value problem (3) and to consider u_ε for $\varepsilon \to 0$. For technical reasons let us consider the following regularized PDE

$$(5) \qquad \dot{u}_\varepsilon + u_\varepsilon \nabla_\Gamma \cdot v + \nabla_\Gamma \cdot f(\cdot, u_\varepsilon) - \varepsilon \nabla_\Gamma \cdot (B \nabla_\Gamma u_\varepsilon) = 0$$

on G_T with initial data $u_\varepsilon = u_{0\varepsilon}$ on Γ_0. $B = B(x, t)$ is a symmetric diffusion matrix which maps the tangent space into the tangent space at the point $x \in \Gamma(t)$, so that we have $B\nu = 0$ and $\nu^* B = 0$. Assume also that B is positive definite on the tangent space and that B satisfies a suitable matrix ODE. It can be shown similarly as in Lemma 0.2 that u is an entropy solution if $u_\varepsilon \to u$. Now we can prove the following a priori estimates.

Lemma 0.4. *Assume that u solves the regularized PDE (5). Then*

$$(6) \qquad \sup_{t \in (0,T)} \|u_\varepsilon(\cdot, t)\|_{L^\infty(\Gamma(t))} \le c, \ \sup_{(0,T)} \int_\Gamma |\nabla_\Gamma u_\varepsilon| \le c, \ \sup_{(0,T)} \int_\Gamma |\dot{u}_\varepsilon| \ \le \ c$$

with a constant c which does not depend on ε.

For the proof we generalize the ideas from the Euclidean case (see [4]) to manifolds. But due to the moving surface the arguments are much more delicate. These estimates imply boundedness of u_ε in $H^{1,1}(G_T)$ and the theorem of Kondrakov compactness in $L^1(G_T)$. Therefore there exists an $u \in L^1(G_T)$ and a subsequence $u_{\varepsilon'}$ which converges to u in $L^1(G_T)$. Then assuming that a smooth solution of (5) exists and using Lemma 0.2 we obtain existence of an entropy solution of (1), (2). Uniqueness follows by the technique of doubling the variables [7] on manifolds.

Now we briefly describe the design of a numerical scheme. Following [5] the smooth initial surface Γ_0 is approximated by a triangulated surface $\Gamma_{0,h}$ which consists of a set of simplices such that all its vertices $\{x_j^0\}_{j=1}^N$ sit on Γ_0. It defines a triangulation $\mathcal{T}_h^0$ of $\Gamma_{0,h}$ and h indicates the maximal diameter of a simplex on the whole family of triangulations. The triangulation $\mathcal{T}_h(t)$ and its $\Gamma(t)$ approximating surface $\Gamma_h(t)$ is defined by the vertices $x_j(t) := \Phi(x_j^0, t)$. Then we have $\mathcal{T}_h(t) = \{T_j(t) | j = 1, \ldots, M\}$ for $t \in [0, T]$, where M is the time independent number of simplices. For the derivation of a finite volume scheme we introduce discrete time steps $t^k = k\tau$ where τ denotes the time step size and k the time step index. For an arbitrary time step t^k we have a smooth surface $\Gamma^k := \Gamma(t^k)$, its approximation $\Gamma_h^k := \Gamma_h(t^k)$ and the corresponding triangulation $\mathcal{T}_h^k := \mathcal{T}_h(t^k)$ with simplices $T_j^k := T_j(t^k)$. By [5] we know that for sufficiently small h there is a uniquely defined lifting operator from Γ_h^k onto Γ^k via the orthogonal projection $\mathcal{P}^k = \mathcal{P}(t^k)$ in direction of the surface normal ν on Γ^k. For the comparison of quantities on Γ^k and on Γ_h^k we define curved simplices via the projection operator, i.e. $\mathfrak{T}_j^k := \mathcal{P}^k T_j^k$. We denote by V_j^k the n-dimensional measure of T_j^k and the finite volume scheme

by

$$(7) \quad u_j^{k+1} := \frac{1}{V_j^{k+1}} \left(V_j^k u_j^k - \tau \sum_{e \subset \partial T_j^k} g_{e,T_j^k}^k(u_j^k, u_{l(j,e)}^k) \right), \quad u_j^0 := \frac{1}{V_j^0} \int_{\mathfrak{T}_j^k} u_0$$

where $g_{e,T_j^k}^k(u_j^k, u_{l(j,e)}^k)$ is a consistent, conservative numerical flux. Here $l(j,e)$ denotes the index of the neighboring simplex of T_j^k due to the edge e. As an example consider the Engquist-Osher numerical flux:

$$(8) \qquad c_{e,T_j^k}^k(u) := \int_e f(\cdot, t^k, u) \cdot \nu_{\partial T_j^k},$$

$$(9) \qquad c_{e,T_j^k}^{k,+}(u) := c_{e,T_j^k}^k(0) + \int_0^u \max\{c_{e,T_j^k}^k{}'(s), 0\} ds,$$

$$(10) \qquad c_{e,T_j^k}^{k,-}(u) := \int_0^u \min\{c_{e,T_j^k}^k{}'(s), 0\} ds,$$

$$(11) \qquad g_{e,T_j^k}^{k,\mathrm{EO}}(u,v) := c_{e,T_j^k}^{k,+}(u) + c_{e,T_j^k}^{k,-}(v).$$

The most interesting numerical test case which we have considered consists of a time dependent, shrinking ellipsoid. On the initial surface we prescribe initial data with compact support (see Figure 1, $t = 0$). Then a shock is moving to the right (see Figure 1, $t = 0.50T$). During the further time evolution the ellipsoid shrinks much faster than before and the mass on the surface is compressed (see Figure 1, $t = 0.58$) and a new discontinuity is created, which moves also to the right (see Figure 1, $t = 0.62T$ up to $t = 0.91T$).

References

[1] Amorim, P., Ben-Artzi, M., LeFloch, P.G., *Hyperbolic conservation laws on manifolds. Total variation estimates and the finite volume method*, Meth. Appli. Anal. **12** (2005), 291-324.

[2] Ben-Artzi, M., LeFloch, P.G., *Well-posedness theory for geometry-compatible hyperbolic conservation laws on manifolds*, Ann. Inst. Henri Poincaré, Anal. Non Linéaire **24**, 989-1008 (2007).

[3] Calhoun, D.A., Helzel, C., LeVeque, R.J., *Logically Rectangular Grids and Finite Volume Methods for PDEs in Circular and Spherical Domains*, SIAM Review **50** (2008), 723-752.

[4] Dafermos, C.M., *Hyperbolic conservation laws in continuum physics*, volume **325** of *Grundlehren der Mathematischen Wissenschaften [Fundamental Principles of Mathematical Sciences]*. Springer-Verlag, Berlin, third edition, 2010.

[5] Dziuk, G., Elliott, C., *Finite elements on evolving surfaces*, IMA Journal Numerical Analysis **25** (2007) 385–407.

[6] Kröner, D., Müller, T., *Related Problems for TV-Estimates for Conservation Laws on Surfaces*, accepted for Hyperbolic problems. Theory, numerics and applications, Proceedings of the 13th international conference on hyperbolic problems, 2010, Peking.

[7] Kružkov, S.N., *First order quasilinear equations with several independent variables*, Mat. Sb. (N.S.), **81** (123):228–255, 1970.

[8] LeFloch, P.G., Neves, W., Okutmustur, B., *Hyperbolic conservation laws on manifolds. Error estimate for finite volume schemes*, Acta Math. Sin., Engl. Ser. **25**, No. 7, 1041-1066 (2009).

(a) t=0

(b) t=0.50T

(c) t=0.58T

(d) t=0.62T

(e) t=0.73T

(f) t=0.91T
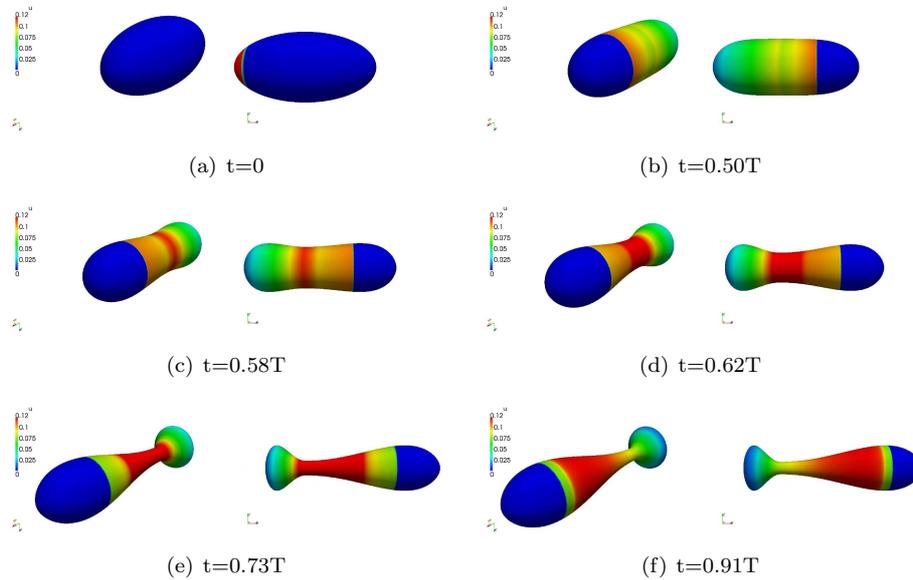
FIGURE 1

[9] Lenz, M., Nemadjieu, S.F., Rumpf, M., *A convergent finite volume scheme for diffusion on evolving surfaces. SIAM Journal on Numerical Analysis*, **49(1)**, 15-37, 2011.
[10] Rossmanith, J. A., Bale, D.S., *LeVeque, R.J., A wave propagation algorithm for hyperbolic systems on curved manifolds*, J. Comput. Phys. **199** (2004), pp. 631-662.

Adaptive Finite Element Methods for the Laplace-Beltrami Operator

ANDREA BONITO

(joint work with J. Manuel Cascón, Khamron Mekchay, Pedro Morin, Ricardo H. Nochetto)

Elliptic partial differential equations on surfaces are ubiquitous from geometry and relativity theory to applications in phase transitions, materials science, and image processing. They are typically governed by the Laplace-Beltrami operator $-\Delta_\gamma$, but more general operators arise as well.

We present and analyze a new adaptive finite element method (AFEM) for the Laplace-Beltrami problem

$$(1) \qquad\qquad -\Delta_\gamma u = f \quad \text{in} \quad \gamma, \qquad u = 0 \quad \text{on} \quad \partial\gamma.$$

Here $\gamma \subset \mathbb{R}^{d+1}$, $d = 1, 2$, is a parametric globally Lipschitz, piecewise W_p^2 hyper surface with $p > d$. The right hand side $f \in L^2(\gamma)$ is assumed to satisfy the compatibility condition $\int_\gamma f = 0$ whenever γ is a closed surface.

Two different types of errors arise when approximating (1) using finite elements: the geometric error due to the approximation of the surface γ by a continuous

piecewise polynomial surface Γ and the error corresponding to the finite element resolution of the partial differential equation (1) on the approximate surface Γ. The nonlinear interplay between these two errors plays a critical role the AFEM needs to accommodate for.

The new algorithm is based on successive applications of two modules, GE-OMETRY and PDE, reducing each component of the error independently. The nonlinear effect is then handled by imposing that the two modules deliver approximations with comparable (properly scaled) errors at each iteration.

The GEOMETRY module relies on a Greedy-type algorithm [1] to improve the geometric approximation in W_∞^1. We show that this procedure delivers optimal decay rates for the geometric error in terms of degrees of freedom.

The PDE module consists in sub-iterations of the standard adaptive loop

$$\text{SOLVE} \to \text{ESTIMATE} \to \text{MARK} \to \text{REFINE}.$$

On a given grid, SOLVE compute the finite element approximation of (1), see [5], ESTIMATE computes the residual type estimator derived in [6], MARK selects a set of cells accounting for a large part of the error using a bulk chasing criteria [4] and REFINE refines the marked cells and possibly others if conforming grids are desired. In the spirit of [3, 2], we prove a contraction property for the sum of the energy error and the scaled residual error estimator between two consecutive adaptive loops.

The optimality of GEOMETRY and the contraction property induced by PDE are instrumental to obtain our main result. *The new AFEM yields a decay rate of energy error plus oscillation in terms of number of degrees of freedom as dictated by the best approximation for this combined nonlinear quantity.*

References

[1] P. Binev, W. Dahmen, R. DeVore and P. Petrushev, *Approximation classes for adaptive methods*, Serdica Math. J., **28(4)** (2002), 391–416.

[2] A.. Bonito and R.H. Nochetto, *Quasi-optimal convergence rate of an adaptive discontinuous Galerkin method*, SIAM J. Numer. Anal., **48** (2010), 734–771.

[3] J.M. Cascón and Ch. Kreuzer, R.H. Nochetto, and K. Siebert, *Quasi-optimal convergence rate for an adaptive finite element method*, SIAM J. Numer. Anal., **46** (2008), 2524–2550.

[4] W. Dörlfer, *A convergent adaptive algorithm for Poisson's equation*, SIAM J. Numer. Anal., **33** (1996), 1106–1124.

[5] G. Dziuk, *Finite Elements for the Beltrami operator on arbitrary surfaces*, Lecture Notes in Math., **1357** (1988), 142–155.

[6] A. Demlow and G. Dziuk, *An adaptive finite element method for the Laplace-Beltrami operator on implicitly defined surfaces*, SIAM J. Numer. Anal., **45** (2007), 421–442.

Mean curvature flow in heterogeneous media
Matteo Novaga
(joint work with Annalisa Cesaroni)

We are interested in the long-time behavior of the mean curvature flow in a periodic heterogeneous medium. The evolution law can be written as a forced mean curvature flow

$$v = \kappa - g$$

where v denotes the inward normal velocity of the evolving hypersurface, κ its mean curvature (with the convention that κ is positive on convex sets) and g is a periodic forcing term. In our model, we assume that the hypersurfaces are graphs with respect to a fixed hyperplane and that the forcing term g does not depend on the variable orthogonal to such hyperplane (fibered medium). Under these assumptions the evolving hypersurface coincides with the graph of the solution to the Cauchy problem

$$(1) \quad \begin{cases} u_t = \sqrt{1 + |Du|^2} \, \mathrm{div} \left(\dfrac{Du}{\sqrt{1 + |Du|^2}} \right) + g\sqrt{1 + |Du|^2} & \text{in } (0, +\infty) \times \mathbb{R}^n \\ u(0, \cdot) = u_0 & \text{in } \mathbb{R}^n. \end{cases}$$

We are particularly interested in the asymptotic behavior as $t \to +\infty$ of solutions to (1), where the initial data u_0 and the forcing term g are assumed to be Lipschitz continuous and $\mathbb{Z}^n$-periodic.

The expected result is that, under appropriate assumptions on g, there exists a unique constant $c \in \mathbb{R}$ and a periodic function ψ such that

$$u(t, y) - ct - \psi(y) \to 0, \qquad \text{as } t \to +\infty, \text{ uniformly in } \mathbb{R}^n.$$

This is a result on the asymptotic stability of special solutions to (1), called traveling wave solutions, which are of the form $\psi + ct$. The constant c and the function ψ are respectively the propagation speed and the profile of the wave.

The first question we address is about the existence of traveling wave solutions to (1). We provide a construction of such solutions using a variational approach developed in [11, 12]. In particular, our solutions are critical points of appropriate functionals, which are exponentially weighted area functionals with a volume term, depending on the speed of propagation c. Exploiting this variational structure, we show existence of traveling waves under rather weak assumptions on the forcing term g, i.e.

$$\exists A \subseteq (0,1)^n \text{ s.t. } \int_A g(y) \, dy > \mathrm{Per}(A, \mathbb{T}^n)$$

where $\mathrm{Per}(A, \mathbb{T}^n)$ is the periodic perimeter of A. Notice that, if $\int_{(0,1)^n} g > 0$, then the previous condition holds true by taking $A = (0,1)^n$.

As our solutions are in general not globally defined, we call them *generalized traveling waves*. We discuss the regularity of these solutions and of their support,

and we list some stronger conditions on the forcing term, involving only the oscillation and the norm of g, under which we show existence of classical traveling waves.

We point out that the variational method selects the *fastest* traveling waves for (1) which are bounded above, in particular it is uniquely defined the speed of propagation $\bar{c}$ of such waves and it holds $\bar{c} \geq \int_{(0,1)^n} g$.

We recall that the problem of existence of classical traveling waves for the forced mean curvature flow has already been considered in the literature, under different assumptions on the forcing term [9, 8, 6]. We also mention [10], where the authors construct V-shaped traveling waves in the whole space for a constant forcing term (see also [14, 5, 4] for similar results in the planar case). The construction of the traveling fronts in these papers relies mainly on maximum principle type arguments, while we use here a variational approach.

The second question of interest is about the convergence, as $t \to +\infty$, of the solution to (1) to a traveling wave solution. We point out that the long-time behavior of solutions of parabolic problems using viscosity solutions type arguments has been extensively considered in the literature: see [13, 3] for the case of quasilinear parabolic problems in periodic environments, and [7] for the case of uniformly parabolic operators in bounded domains with Neumann boundary conditions. However, none of these results applies to mean curvature type equations such as (1). We will describe the asymptotic behavior as $t \to +\infty$ of the maximum of the function $u(t, \cdot)$. Namely, letting $Q := (0, 1)^n$, we show that there exists a constant $K > 0$ such that

$$\min_{Q} u_0 + \bar{c}t \leq \max_{Q} u(t, y) \leq \bar{c}t + K + \frac{\log(1 + t)}{\bar{c}}.$$

We also show that, along a subsequence $t_n \to +\infty$,

$$u(t_n, y) - \max_{Q} u(t_n, \cdot) \longrightarrow \begin{cases} \psi(y) & \text{locally in } C^{1+\alpha}(E) \\ -\infty & \text{locally uniformly in } Q \setminus \overline{E} \end{cases}$$

for all $\alpha \in (0, 1)$, where $\psi + \bar{c}t$ is a generalized traveling wave supported in $E \subset Q$.

We point out that the proof of the convergence result, as well as the proof of existence of generalized waves, essentially uses variational methods, rather than maximum principle based argumets.

References

[1] G. Barles, S. Biton, M. Bourgoing, O. Ley, *Uniqueness results for quasilinear parabolic equations through viscosity solutions methods*, Calc. Var. Partial Differential Equations, **18** (2003), 159–179.

[2] G. Barles, A. Cesaroni, M. Novaga, *Homogenization of fronts in highly heterogeneous media*, SIAM J. Math. Anal. **43** (2011), 212–227.

[3] G. Barles, P. E. Souganidis, *Space-time periodic solutions and long-time behavior of solutions to quasi-linear parabolic equations*, SIAM J. Math. Anal. **32** (2001), 1311–1323.

[4] L. Bendong, *Periodic traveling waves of a mean curvature flow in heterogeneous media*, Discrete Contin. Dyn. Syst. **25** (2009), 231–249.

[5] L. Bendong, X. Chen, *Traveling waves of a curvature flow in almost periodic media*, J. Differential Equations **247** (2009), 2189–2208.

[6] P. Cardaliaguet, P.-L. Lions, P.E. Souganidis, *A discussion about the homogenization of moving interfaces*, J. Math. Pures Appl. **91** (2009), 339–363.

[7] F. Da Lio, *Large time behavior of solutions to parabolic equations with Neumann boundary conditions*, J. Math. Anal. Appl. **339** (2008), 384–398.

[8] N. Dirr, G. Karali, N.K. Yip, *Pulsating wave for mean curvature flow in inhomogeneous medium*, European J. Appl. Math. **19** (2008), 661–699.

[9] P.-L. Lions, P. E. Souganidis, *Homogenization of degenerate second-order PDE in periodic and almost periodic environments and applications*, Annales IHP - Analyse Nonlinéaire **22** (2005), 667–677.

[10] R. Monneau, J.M. Roquejoffre, V. Roussier-Michon, *Travelling graphs for the forced mean curvature motion in an arbitrary space dimension*, Preprint (2011).

[11] C. Muratov, *A global variational structure and propagation of disturbances in reaction-diffusion systems of gradient type*, Discrete Cont. Dyn. Syst. B **4** (2004), 867–892.

[12] C. Muratov, M. Novaga, *Front propagation in infinite cylinders. II. The sharp reaction zone limit*, Calc. Var. Partial Differential Equations **31** (2008), 521–547.

[13] G. Namah, J.M. Roquejoffre, *Convergence to periodic fronts in a class of semilinear parabolic equations*, Nonlinear Differential Equations Appl. **4** (1997), 521–536.

[14] H. Ninomiya, M. Taniguchi, *Stability of traveling curved fronts in a curvature flow with driving force*, Methods Appl. Anal. **8** (2001), 429–450.

Degenerate Neckpinches in Ricci flow: Numerics to Matched Asymptotics to Theorems

JAMES ISENBERG

(joint work with Sigurd Angenent, David Garfinkle, Dan Knopf)

The study of degenerate neckpinches in Ricci flow has provided an archetypal example of the important role which numerical simulation can play in geometric analysis. While some of the features of degenerate neckpinch formation had been predicted by Hamilton and others back in the 1980's, the numerical exploration of these phenomena (done by two of the authors) has provided crucial insight into their behavior. Based on these numerical explorations, three of the authors have carried out a formal matched asymptotics analysis of degenerate neckpinches, thereby obtaining very detailed information concerning their geometric nature. We are currently working to prove that degenerate neckpinches, with the explicit behavior explored in both the numerical and the matched asymptotic studies, do indeed develop during Ricci flow starting from certain types of initial data.

Ricci flow evolves any specified initial metric $\hat{g}$ on a fixed manifold M^n via the flow equation

$$(1) \qquad\qquad \partial_t g(t) = -2Rc[g(t)] + \nu g(t),$$

(with $g(0) = \hat{g}$) where ν is a normalization function. It has been shown (using parabolic flows related to Ricci flow by time-dependent diffeomorphism) that the Ricci flow initial value problem is well-posed [2], and that the flow extends in time so long as the curvature is bounded [3].

To study particular examples of Ricci flows which develop degenerate neckpinches, we consider one-parameter families $\hat{g}_{[\lambda]}$ of initial geometries on $M^n = S^3$ with rotationally symmetric "corsetting" about the equator. The parameter λ

labels the relative tightness of the corsetting, with larger values of λ indicating tighter corsetting. For a number of these one-parameter families of initial geometries, we have numerically simulated [5, 6] the volume-normalized Ricci flows which start at several initial geometries (for a wide range of values of λ), and have found the following: Those flows starting at geometries with relatively loose corsetting ($\lambda < \lambda_c$, for some "critical" λ_c) evolve towards rounder and rounder metrics, and ultimately converge to the completely round three-sphere metric, while those flows starting at geometries with relatively tighter corsetting ($\lambda > \lambda_c$) evolve to develop nondegenerate neckpinches at the equator, characterized by the curvature blowing up in finite time as the equator circumference shrinks to zero (and the flow stops).

Noting the qualitatively very different behavior of the flows starting at geometries with corsetting looser or tighter than λ_c, we are led to ask what happens to normalized Ricci flow which starts at a threshold initial geometry $\hat{g}_{[\lambda_c]}$. It is these which develop degenerate neckpinches, and are of primary interest for this research program.

Before describing the behavior seen in the flows starting at threshold geometries $\hat{g}_{[\lambda_c]}$, we recall that a particular Ricci flow is said to develop a singularity if there is a finite time T_s such that as $t \to T_s$, the curvature of the evolving metric $g(t)$ is unbounded. Such a singularity is called a *neckpinch singularity* if, roughly speaking, in the neighborhood of a spatial point $x_s \in M^n$ at which the curvature becomes unbounded, the limit of the flows for a sequence of localized curvature-renormalized metric dilations[1] forms a cylinder. A neckpinch singularity at x_s is defined to be *nondegenerate* if the limits of all curvature-normalizing metric dilations arbitrarily close to x_s lead to cylinders, and it is defined to be *degenerate* if this is not the case.

Classifying a different aspect of Ricci flow singularities, one labels a singularity to be *Type I* if it is rapidly forming in the sense that $|T_s - t|sup_{x \in M^n}|Rm[g(x,t)]|$ is bounded, while the singularity is labeled *Type II* if it is slowly forming in the sense that $|T_s - t|sup_{x \in M^n}|Rm[g(x,t)]|$ is unbounded.

While the inherent nature of numerical simulations makes it impossible to identify the threshold initial geometry $\hat{g}_{[\lambda_c]}$ with complete accuracy, we can effectively explore the behavior of the Ricci flow $g_{[\lambda_c]}(t)$ which evolves from $\hat{g}_{[\lambda_c]}$ by numerically simulating the Ricci flows for a sequence of initial geometries $\hat{g}_{[\lambda_i]}$ with λ_i approaching closer and closer to λ_c, both from above and below. We carry out this program in [5, 6], thereby observing the following features of the threshold flows: 1) The flows form "javelins", in the sense that the curvature peaks at the tips (poles), while the geometry elsewhere approximates a cylinder. 2) The flows develop singularities at the tips, which are degenerate neckpinches. 3) In a neighborhood of the tips, the flows locally approach "Bryant solitons", which are

---

[1]The process of studying the limits of flows for sequences of local curvature-normalizing dilations of the metric is made precise using the notion of "singularity models"; see, e.g., [4].

rotationally symmetric steady gradient solitons.[2] 4) The rate of curvature blowup is Type II.

The work of Gu and Zhu [7], subsequent to this numerical work, proves that the Ricci flows of threshold-type geometries generally develop Type II singularities which are degenerate neckpinches. Their work does not, however, tell us very much about the detailed behavior of these flows. Based on what we have learned from our numerical studies, we have explored some of these details by using the tools of "formal matched asymptotics" to argue strongly that there is a large class of threshold flow solutions with a well-understood evolution (including the four features noted above)[1]. We believe that we will soon be able to complete a proof that these solutions exist.

The idea of a formal matched asymptotics study is roughly as follows: Starting with the set of equations $\mathcal{F}[\psi] = 0$ governing the evolution of the system being studied, one presumes that for the class of solutions which one seeks to explore (during the time frame of interest), certain terms in the equations $\mathcal{F}[\psi] = 0$ dominate certain others. Dropping the dominated terms to form the simplified system $\hat{\mathcal{F}}[\psi] = 0$, one obtains solutions $\hat{\psi}$ of the simplified system, and then one uses $\hat{\psi}$ as an expansion basis for approximate solutions of the original system. One checks consistency by studying if the terms which have been dropped in going from $\mathcal{F}[\psi]$ to $\hat{\mathcal{F}}[\psi]$ are indeed negligible for solutions ψ which are close to $\hat{\psi}$.

We carry out such an analysis (in [1]) for the normalized Ricci flow equations for rotationally symmetric metrics on $S^n (n \geq 3)$ satisfying a collection of assumptions which correspond to the formation of a degenerate neckpinch singularity in a neighborhood of one of the poles. This analysis leads us to conjecture the existence of a family of solutions–parametrized by an integer $k \geq 3$–which form neckpinch singularities with curvature blowup at the rate $sup_{x \in S^3}|Rm[g(x,t)]| \sim \frac{C}{(T_s-t)^{2-\frac{2}{k}}}$ (consistent with the singularities being Type II). For all of these conjectured solutions, we describe explicitly what the behavior of the geometry is near the developing singularity, including the asymptotic approach to a Bryant soliton at the pole.

We hope to soon have a proof that solutions of the conjectured form do in fact exist.

In future work, we plan to study the development of degenerate neckpinches in Ricci flow which are not rotationally symmetric. We note that the numerical study of these flows is likely to be challenging, since they involve the evolution of geometric quantities on manifolds which are not patches of R^n. We note that for rotationally symmetric flows, the spatial manifold effectively reduces to an interval in R^1.

---

[2]A steady gradient soliton metric g satisfies the condition $Rc[g] + \nabla\nabla f = 0$ for some function f; it follows that the Ricci flow for g evolves purely by diffeomorphism.

References

[1] S. Angenent, J. Isenberg and D. Knopf *Formal matched asymptotics for degenerate Ricci flow neckpinches*, Nonlinearity **24** (2011), 2265-2280.

[2] D. DeTurck, *Deforming metrics in the direction of their Ricci tensors*, J. Differential Geom. **18** (1983) 157-162.

[3] R. Hamilton, *Three-manifolds with positive Ricci curvature*, J. Differential Geom. *17* (1982), 255-306.

[4] R. Hamilton, *The formation of singularities in the Ricci flow* , Surveys in Differential Geometry Vol II (Cambridge, MA, 1993), 7-136.

[5] D. Garfinkle and J. Isenberg *Numerical studies of the behavior of Ricci flow*, Contemp. Math. **367** (2005), 103–114.

[6] D. Garfinkle and J. Isenberg *The modeling of degenerate neckpinch singularities in Ricci flow by Bryant solitions* J. Math. Phys. **49** (2008) 073505.

[7] H-L Gu and X-P Zhu *The existence of Type II singularities for the Ricci flow on S^{n+1}* Commun. Anal. Geom. **16** (2008) 467-494.

Finite element approximation of large bending isometries
Sören Bartels

1.1. **Mathematical model for plate bending.** The elastic bending of a thin plate can be derived from three-dimensional hyperelasticity and leads to a minimization of the energy functional

$$E(y) = \frac{\alpha}{2} \int_\Omega |II|^2 \, \mathrm{d}x - \int_\Omega f \cdot y \, \mathrm{d}x$$

with the second fundamenal form $II = (\partial_i b \cdot \partial_j y)_{ij}$, $b = \partial_1 y \times \partial_2 y$, under the constraint that y is an isometry, i.e., that for the first fundamental form $I = (\partial_i y \cdot \partial_j y)_{ij}$ we have $I = I_2$ in Ω with the identity matrix $I_2 \in \mathbb{R}^{2 \times 2}$, and subject to the boundary conditions $y = y_\mathrm{D}$ and $\nabla y = \Phi_\mathrm{D}$ on $\Gamma_\mathrm{D} \subset \partial\Omega$. Imposing a condition on ∇y on Γ_D is equivalent to prescribing the normal b of the deformed plate on Γ_D. The model has recently been rigorously justified in [7] and coincides with the model proposed in [9]. As a consequence of Gauss's *theorema egregium* we have for a C^2 isometry $y : \Omega \to \mathbb{R}^3$ that the Gaussian curvature K vanishes and that

$$|II|^2 = 4H^2 = |\Delta y|^2 = |D^2 y|^2$$

with the mean curvature H. The density results for smooth isometries among isometries in $H^2(\Omega; \mathbb{R}^3)$ proved in [8] show that for an isometry $y \in H^2(\Omega; \mathbb{R}^3)$ we have the same identities and this allows us to replace the Frobenius norm of the second fundamental form of the surface parametrized by y by the Frobenius norm of the Hessian of y.

1.2. **Approximation with discrete Kirchhoff triangles.** Given a triangulation $\mathcal{T}_h$ of Ω a discrete Kirchhoff triangle defines a linear mapping $\theta_h : W_h \to \Theta_h$ that serves as an approximation of the gradient. In [5] the space $W_h \subset H^1(\Omega)$ consists of continuous functions that are reduced cubic polynomials on each element such that their gradients are continuous at the vertices of elements and the space $\Theta_h \subset H^1(\Omega)$ contains continuous, piecewise quadratic vector fields whose normal derivative is linear along every side of an element. The operator θ_h enables us to define an approximate Hessian by $\nabla\theta_h(w_h)$. If $\mathcal{N}_h$ denotes the set of vertices of elements and $\mathcal{I}_h$ the nodal interpolation operator onto the space of continuous, piecewise affine finite elements, we consider the following finite-dimensional constrained minimization problem:

(1)
$$
\begin{cases}
\text{Minimize } y_h \mapsto E_h(y_h) = \dfrac{\alpha}{2}\int_\Omega |\nabla\theta_h(y_h)|^2 \, \mathrm{d}x - \int_\Omega \mathcal{I}_h[f_h \cdot y_h] \, \mathrm{d}x \\
\text{subject to } y_h \in W_h^3 \text{ and } [\nabla y_h(z)]^T \nabla y_h(z) = I_2 \text{ for all } z \in \mathcal{N}_h, \\
\text{and } y_h(z) = y_D(z), \ \nabla y_h(z) = \Phi_D(z) \text{ for all } z \in \mathcal{N}_h \cap \Gamma_D.
\end{cases}
$$

Notice that only the *independent* nodal values $\big(y_h(z) : z \in \mathcal{N}_h\big)$ and $\big(\nabla y_h(z) : z \in \mathcal{N}_h\big)$ are required for the implementation. By interpolation of a smooth, nearly minimizing isometry it can be shown that discrete minimizers accumulate at minimizing isometries in $H^2(\Omega;\mathbb{R}^3)$, cf. [4] for details. Stationary points of E_h can be found by employing a discrete H^2 gradient flow of the energy functional with a linearization of the nodal isometry constraint about the current iterate. More precisely, given an approximation $y_h^n \in W_h^3$ we define

$$
F_h[y_h^n] = \big\{ w_h \in W_h^3 : [\nabla w_h(z)]^T \nabla y_h^n(z) + [\nabla y_h^n(z)]^T \nabla w_h(z) = 0 \text{ for all } z \in \mathcal{N}_h
$$
$$
\text{and } w_h(z) = 0, \ \nabla w_h(z) = 0 \text{ for all } z \in \mathcal{N}_h \cap \Gamma_D \big\}
$$

and compute for $\tau > 0$ the correction $d_t y_h^{n+1} \in F_h[y_h^n]$ as the solution of

(2) $\big(\nabla\theta_h(d_t y_h^{n+1}), \nabla\theta_h(z_h)\big) + \alpha\big(\nabla\theta_h(y_h^n + \tau d_t y_h^{n+1}), \nabla\theta_h(z_h)\big) = \big(f_h, z_h\big)_h$

for all $z_h \in F_h[y_h^n]$. The new iterate is defined by $y_h^{n+1} = y_h^n + \tau d_t y_h^{n+1}$. In (2), $(\cdot,\cdot)$ denotes the L^2 inner product with corresponding norm $\|\cdot\|$ and $(v,w)_h = \int_\Omega \mathcal{I}_h[vw] \, \mathrm{d}x$. This iteration is unconditionally stable and energy decreasing in the sense that for all $n \geq 0$ we have

(3) $E_h(y_h^{n+1}) + \dfrac{\tau}{2}\|\nabla\theta_h(d_t y_h^{n+1})\|^2 \leq E_h(y_h^n).$

The iterates (y_h^n) will in general not satisfy the nodal isometry constraint but provided that the initial deformation y_h^0 satisfies $\big[\nabla y_h^0(z)\big]^T \nabla y_h^0(z) = I_2$ for all $z \in \mathcal{N}_h$ we have that, cf. [4],

(4) $\|\mathcal{I}_h[\nabla y_h^n]^T \nabla y_h^n - I_2\|_{L_h^1(\Omega)} \leq C\tau E_h(y_h^0).$

1.3. **Reissner-Mindlin approximation.** A different approach to the finite element approximation of bending isometries consists in relaxing the second order derivatives on the continuous level by introducing the additional variable $\Phi \approx \nabla y$ and adding a penalty term to the energy functional, i.e., the minimization of

$$E_t(\Phi, y) = \frac{t^{-2}}{2} \|\Phi - \nabla y\|^2 + \frac{\alpha}{2} \int_\Omega |\nabla \Phi|^2 \, \mathrm{d}x - \int_\Omega f \cdot y \, \mathrm{d}x$$

subject to the conditions $y|_{\Gamma_\mathrm{D}} = y_\mathrm{D}$, $\Phi|_{\Gamma_\mathrm{D}} = \Phi_\mathrm{D}$, and $\Phi^T \Phi = I_2$ in Ω. For the minimization of E_t we employ a discrete H^1 gradient flow of E_t with respect to Φ, i.e., we consider the time-incremental evolution defined by the successive minimization of the functionals

$$E_t^n(\Phi, y) = \frac{1}{2\tau} \|\nabla(\Phi - \Phi^{n-1})\|^2 + \frac{t^{-2}}{2} \|\Phi - \nabla y\|^2 + \frac{\alpha}{2} \int_\Omega |\nabla \Phi|^2 \, \mathrm{d}x - \int_\Omega f \cdot y \, \mathrm{d}x,$$

where Φ^{n-1} is the solution from the previous time step and $\tau > 0$ the time-step size. The condition that Φ satisfies $\Phi^T \Phi = I_2$ is in the minimization of E_t^n replaced by the linearized condition

$$(\Phi - \Phi^{n-1})^T \Phi^{n-1} + \Phi^{n-1,T}(\Phi - \Phi^{n-1}) = 0,$$

To avoid locking effects in the numerical solution of the linear problems in each time step for small parameters $t > 0$, we extend a finite element method developed in [1] for the approximation of linear Reissner-Mindlin models for small displacements. The spaces and the discretization of E_t^n are chosen in such a way that the difference $t^{-2}(P_0 \Phi_h^n - \nabla_h y_h^n)$ allows a discrete Helmholtz decomposition. The main part in the solution of one time-step then consists in the solution of a problem that is similar to a discretized Stokes system. An energy decreasing property and convergence of discrete minimizers can be shown on weakly acute triangulations under the conditions $\tau \leq Ch^{2/3}$ and $th^{-1} \leq C$. We refer the reader to [3] for details.

1.4. **Experiment with compressive boundary conditions.** A small vertical load selects one of at least two possible solutions related to the symmetry in vertical direction in the case of compressive boundary conditions at the ends of a rectangular plate for $f = 0$. Figure 1 shows the numerical solution obtained with a Reissner-Mindlin approximation on a triangulation with mesh-size $h \sim 2^{-4}$ and $t = h/4$. Similar deformations were computed with discrete Kirchhoff triangles. For details and other experiments we refer the reader to [3, 4].

REFERENCES

[1] ARNOLD, D. N., AND FALK, R. S. A uniformly accurate finite element method for the Reissner-Mindlin plate. *SIAM J. Numer. Anal. 26*, 6 (1989), 1276–1290.

[2] BARTELS, S. Numerical analysis of a finite element scheme for the approximation of harmonic maps into surfaces. *Math. Comp. 79*, 271 (2010), 1263–1301.

[3] BARTELS, S. Finite element approximation of large bending isometries. Preprint, 2011.

[4] BARTELS, S. Approximation of large bending isometries with discrete Kirchhoff triangles. Preprint, 2011.
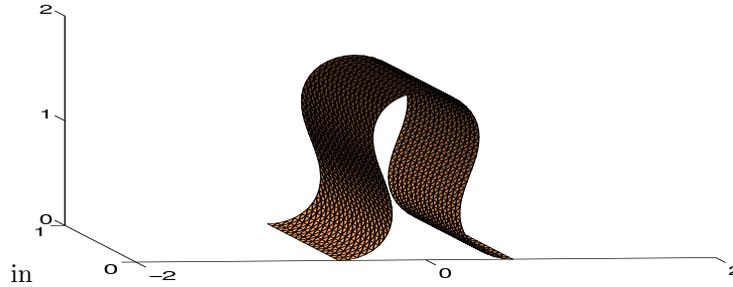
FIGURE 1. Numerical solution for 70.0% compression of a 4×1 plate colored by discrete mean curvature.

[5] BATOZ, J.-L., BATHE, K.-J., AND HO, L.-W. A study of three-node triangular plate bending elements. *International Journal for Numerical Methods in Engineering 15*, 12 (1980), 1771–1812.

[6] BRAESS, D. *Finite elements*. Cambridge University Press, Cambridge, 2007.

[7] FRIESECKE, G., JAMES, R. D., AND MÜLLER, S. A theorem on geometric rigidity and the derivation of nonlinear plate theory from three-dimensional elasticity. *Comm. Pure Appl. Math. 55*, 11 (2002), 1461–1506.

[8] HORNUNG, P. Approximating $W^{2,2}$ isometric immersions. *C. R. Math. Acad. Sci. Paris 346*, 3-4 (2008), 189–192.

[9] KIRCHHOFF, G. R. Über das Gleichgewicht und die Bewegung einer elastischen Scheibe. *J. Reine Angew. Math. 40* (1850), 51–88.

Convex minimization and phase field models

CARSTEN GRÄSER

(joint work with Ralf Kornhuber, Uli Sack)

We are interested in the efficient numerical solution of the anisotropic Allen–Cahn equation

$$\varepsilon \langle u_t, v - u \rangle + \varepsilon \Big((\gamma^2)'(\nabla u), \nabla(v - u) \Big) + \phi(v) - \phi(u) \geq \frac{1}{\varepsilon}(u, v - u)$$

on $\Omega \times (0, T)$ for a bounded domain $\Omega \subset \mathbb{R}^d$. This equation is obtained as scaled L^2-gradient flow for the Ginzburg–Landau free energy

$$\mathcal{E}(u) = \frac{\varepsilon}{2} \int_\Omega \gamma^2(\nabla u) \, dx + \frac{1}{\varepsilon} \int_\Omega \Phi(u) + \frac{1}{2}(1 - u^2) \, dx, \quad \phi(u) = \frac{1}{\varepsilon} \int_\Omega \Phi(u) \, dx$$

with an anisotropy function $\gamma : \mathbb{R}^d \to \mathbb{R}$ and a double-well potential $\Phi(u) + \frac{1}{2}(1 - u^2)$ with convex part $\Phi : \mathbb{R} \to \mathbb{R} \cup \{\infty\}$. We assume that

- γ is continuous and 1-homogeneous on $\mathbb{R}^d$,
- γ is positive and twice continuously differentiable on $\mathbb{R}^d \setminus \{0\}$,
- the Hessian $(\gamma^2)''$ of γ^2 is symmetric positive definite on $\mathbb{R}^d \setminus \{0\}$,
- Φ is convex, proper, lower semicontinuous, and non-negative,
- $\phi : H^1(\Omega) \to \mathbb{R} \cup \{\infty\}$ is lower semicontinuous.

These assumptions include the well-known logarithmic potential

$$\Phi(u) = \Phi_\theta(u) = \frac{\theta}{2}\Big((1+u)\log(1+u) + (1-u)\log(1-u)\Big)$$

as well as the obstacle potential as its limit for $\theta \to 0$.

Due the parabolic nature of this equation an implicit time discretization is in principle desirable. However fully implicit time discretizations still lead to time-step restrictions because of the concave part in the double-well potential. This issue has been addressed by several authors by semi-implicit time discretizations where the concave part is discretized explicitly in time.

Both, the implicit and semi-implicit discretization, lead to problems of the form

$$\frac{\varepsilon}{\tau}(u - u^{\mathrm{old}}, v - u) + \varepsilon\Big((\gamma^2)'(\nabla u), \nabla(v - u)\Big) + \phi(v) - \phi(u) - \frac{1}{\varepsilon}(\tilde{u}, v - u) \geq 0$$

with $\tilde{u} = u$ and $\tilde{u} = u^{\mathrm{old}}$, respectively, where u^{old} is the solution from the last time step. Compared to the isotropic case these problems are significantly more expensive to solve because the linear differential operator is replaced by a nonlinear one.

In order to overcome this we propose a new time discretization that approximates the anisotropic term by an isotropic one based on

$$\Big((\gamma^2)'(\nabla u), \nabla v\Big) \approx \Big((\gamma^2)'(\nabla u^{\mathrm{old}}), \nabla v\Big) + \lambda(\nabla u - \nabla u^{\mathrm{old}}, \nabla v)$$

for some $\lambda > 0$. This approach is similar to a linearization of $(\gamma^2)'$ where $\lambda\,\mathrm{Id}$ replaces the second derivative of γ^2 that does not exist in general. The resulting stationary problems then take the form

$$\frac{\varepsilon}{\tau}(u - u^{\mathrm{old}}, v - u) + \varepsilon\lambda(\nabla u, \nabla(v - u)) + \phi(v) - \phi(u) - \frac{1}{\varepsilon}(\tilde{u}, v - u)$$
$$\geq \varepsilon\Big(\lambda\nabla u^{\mathrm{old}} - (\gamma^2)'(\nabla u^{\mathrm{old}}), \nabla(v - u)\Big).$$

We refer to these as 'linearized' implicit and semi-implicit discretization.

Theorem 1 (see [5]). *Under the above assumptions the semi-implicit and linearized semi-implicit discretization exhibit a unique solution. The same is true for the implicit and the linearized implicit discretization provided that the time step restriction $\tau < \varepsilon^2$ is satisfied.*

The proof is a straight forward application of standard results for equivalent convex minimization problems whose energy functionals are essentially given by the convex part $\mathcal{E}_0$ of $\mathcal{E}$. Moreover the above assumptions on γ imply that

$$L := \sup_{x,y \in S^{d-1}} (\gamma^2)''(x)y \cdot y, \qquad \mu := \inf_{x,y \in S^{d-1}} (\gamma^2)''(x)y \cdot y$$

are both positive and thus the strong convexity of $\mathcal{E}_0$ and Lipschitz continuity of its gradient with respect to the H^1-seminorm [5, 1]. This property is the key ingredient to establish the following stability results.

Theorem 2 (see [5])**.** *Let $\lambda \geq L/2$. Then the semi-implicit and linearized semi-implicit discretization satisfy the stability estimate*

$$\left(\frac{\varepsilon}{\tau} + \frac{1}{2\varepsilon}\right)\|u - u^{old}\|_0^2 + \frac{\varepsilon\mu}{4}\|\nabla u - \nabla u^{old}\|_0^2 + \mathcal{E}(u) \leq \mathcal{E}(u^{old}).$$

If additionally $\tau < \varepsilon^2$ is satisfied then the implicit and the linearized implicit discretization satisfy the stability estimate

$$\frac{\varepsilon}{2\tau}\|u - u^{old}\|_0^2 + \frac{\varepsilon\mu}{4}\|\nabla u - \nabla u^{old}\|_0^2 + \mathcal{E}(u) \leq \mathcal{E}(u^{old}).$$

As numerical accuracy test we compare the evolution of shrinking Wulff shapes under the time discrete anisotropic Allen–Cahn equations with the analytically known rates for it sharp interface limit (see e.g. [6]). We start the evolution with a single inclusion with Wulff shape like 0-level set in an otherwise pure phase.

For a threefold Kobayashi anisotropy and a regularized l^1-norm given by

$$\gamma(re^{i\alpha}) = (1 + 0.124\cos(3\alpha))|r|, \qquad \gamma(x) = \sum_i \sqrt{x_i^2 + 10^{-3}|x|^2}$$

we observe that all four discretizations reproduce the shrinking Wulff shape. While the shrinking rates are reproduced nicely for the Kobayashi anisotropy by the nonlinear and linearized implicit version, even for $\lambda \geq L/4$, the semi-implicit versions fail to provide a comparable accuracy even below the time step restriction needed for the implicit version.

The situation looks worse for the regularized l^1-norm where the linearized version does not produce reasonable results unless λ is much larger than $L/2$ requiring smaller time steps. In contrast the nonlinear implicit version still works well.

Due to these results a fast solver for stationary problems that is also capable to solve anisotropic problems is needed. We propose to use the *truncated nonsmooth Newton multigrid* (TNNMG) method [4, 2, 1] for adaptive first order finite element discretizations obtained using a hierarchical error estimator [3, 1].

The foundation of this method is the nonlinear Gauß–Seidel iteration that provides global convergence. It is augmented by Newton-like corrections for truncated linear systems. These systems are obtained as linearization of the problem in only those components where it is smooth enough. They can be solved approximately by one step of a standard multigrid algorithm. Subsequent projection of the linear corrections into the feasible set and a line search for the projected corrections lead to an overall monotone nonlinear multigrid method that converges globally [1]. Numerical experiments show that it exhibits mesh independent convergence rates for isotropic and anisotropic stationary problems if solutions from coarser meshes are used as initial iterates. However, the computational cost is much larger for anisotropic problems.

We summarize that the linearized implicit time discretization allows to reduce the computational effort significantly if the anisotropy is moderate. If the anisotropy is close to a nonsmooth anisotropy the linearized discretization will fail and one has to stick with anisotropic stationary problems. For both cases the semi-implicit versions are practically unusable because they do not provide

a reasonable accuracy even if the time step restriction of the implicit version is matched. In any case the TNNMG method allows to solve the stationary problems with multigrid efficiency.

REFERENCES

[1] C. Gräser, *Convex minimization and phase field models*, PhD thesis, Freie Universität Berlin, 2011.
[2] C. Gräser and R. Kornhuber, *Multigrid methods for obstacle problems*, J. Comp. Math., **27** (2009), 1–44. submitted.
[3] C. Gräser, R. Kornhuber, and U. Sack, *On hierarchical error estimators for time-discretized phase field models*, In: Proceedings of ENUMATH 2009, Springer, 2010, 397–406.
[4] C. Gräser, U. Sack, and O. Sander, *Truncated nonsmooth Newton multigrid methods for Convex minimization problems*, In: Domain Decomposition Methods in Science and Engineering XVIII, LNCSE, Springer, 2009, 129–136.
[5] C. Gräser, R. Kornhuber, and U. Sack, *Time discretizations of anisotropic Allen–Cahn equations*, submitted.
[6] Y. Giga, *Surface evolution equations*, Birkhäuser, Basel, 2006.

H^1 **Willmore flow with local area preservation**
BJÖRN STINNER

On the set of smooth, immersed, compact hypersurfaces $\Gamma \subset \mathbb{R}^3$ consider the inner product (which is a weighted H^1 product)

$$\left(\boldsymbol{v}, \boldsymbol{w}\right)_{H^1_{\alpha,\beta}} := \int_\Gamma \alpha \boldsymbol{v} \cdot \boldsymbol{w} + \beta \nabla_\Gamma \boldsymbol{v} : \nabla_\Gamma \boldsymbol{w} \quad \forall \boldsymbol{v}, \boldsymbol{w} : \Gamma \to \mathbb{R}^3.$$

With respect to this inner product we numerically study a gradient flow dynamics of the Willmore energy

$$F_b(\Gamma) = \int_\Gamma \frac{1}{2} |\boldsymbol{\kappa}|^2,$$

where $\boldsymbol{\kappa}$ is the mean curvature vector, but with the additional constraint that the area of each portion of the surface remains preserved. The idea is to resort to the method of [4] for the classical L^2 Willmore flow which is based on surface finite elements and to employ a mixed formulation using quadratic and linear surface finite elements.

Problem: Find a family of hypersurfaces $\{(\Gamma(t))\}_t$ in $\mathbb{R}^3$ with velocity $\boldsymbol{v}(t)$ and mean curvature vector $\boldsymbol{\kappa}(t)$ and find a *tension* field $\sigma(t)$ such that for all test functions $\boldsymbol{w}, \boldsymbol{\psi} : \Gamma \to \mathbb{R}^3$ and $\lambda : \Gamma \to \mathbb{R}$

$$\left(\boldsymbol{v}, \boldsymbol{w}\right)_{H^1_{\alpha,\beta}} = -\left\langle \delta F_b(\Gamma), \boldsymbol{w} \right\rangle - \int_\Gamma \sigma \nabla_\Gamma \cdot \boldsymbol{w},$$

$$\int_\Gamma \lambda \nabla_\Gamma \cdot \boldsymbol{v} = 0.$$

In [4], the variation of the energy is derived making explicit use of the mean curvature vector $\boldsymbol{\kappa}$ and involving only first order surface derivatives. The above

describe problem leads immediately to the question of solvability with respect to the velocity and the tension.

Subproblem: Given a hypersurface Γ and a function $\boldsymbol{f} : \Gamma \to \mathbb{R}^3$, find $\boldsymbol{v} \in V := H^1(\Gamma)$ and $\sigma \in H := L^2(\Gamma)$ such that

$$\int_\Gamma \alpha \boldsymbol{v} \cdot \boldsymbol{w} + \beta \nabla_\Gamma \boldsymbol{v} : \nabla_\Gamma \boldsymbol{w} + \sigma \nabla_\Gamma \cdot \boldsymbol{w} = \int_\Gamma \boldsymbol{f} \cdot \boldsymbol{w} \quad \forall \boldsymbol{w} \in V,$$

$$\int_\Gamma \lambda \nabla_\Gamma \cdot \boldsymbol{v} = 0 \quad \forall \lambda \in H.$$

Solvability of the subproblem follows from the following inf-sup condition (see [1]):

$$\inf_{\lambda \in H} \sup_{\boldsymbol{w} \in V} \frac{\int_\Gamma \lambda \nabla_\Gamma \cdot \boldsymbol{w}}{\|\lambda\|_H \|\boldsymbol{w}\|_V} \geq B > 0.$$

Discretisation: The idea is to use the P2–P1 Taylor-Hood element where the issue then is to investigate whether the convergence analysis from the planar case can be extended to the present case of hypersurfaces, which is work in progress. But if so then one would expect convergence of order two for both $\boldsymbol{v}$ in the V norm and σ in the H norm. In addition to the classical finite element error estimate one will have to deal with an error from the geometric approximation of the hypersurface. But this error is well understood [3]: Quadratic surface finite elements will be sufficient to get optimal orders of convergence, and these have been used in computations that is reported on below.

The following spaces appear in the following numerical experiments:

$$V_h(\Gamma_h) := \left\{ \phi_h \in C^0(\Gamma_h) \,\middle|\, \phi_h \circ \Phi_T \text{ quadratic on } \hat{T} \text{ for all } T \in \mathcal{T}_h \right\},$$

$$H_h(\Gamma_h) := \left\{ b_h \in C^0(\Gamma_h) \,\middle|\, b_h \circ \Phi_T \text{ linear on } \hat{T} \text{ for all } T \in \mathcal{T}_h \right\}.$$

The scheme is based on the approach of [4] on the L^2 Willmore flow.

Scheme: For $m = 1, 2, \ldots$, given Γ_h^m find $\boldsymbol{u}_h^{m+1}, \boldsymbol{\kappa}_h^{m+1} \in V_h(\Gamma_h^m)$ and $\sigma_h^{m+1} \in H_h(\Gamma_h^m)$ such that for all $\boldsymbol{w}_h, \boldsymbol{\psi}_h \in V_h(\Gamma_h^m)$ and $\lambda_h \in H_h(\Gamma_h^m)$

$$\int_{\Gamma_h^m} \frac{\alpha}{\tau^m} \boldsymbol{u}_h^{m+1} \cdot \boldsymbol{w}_h + \frac{\beta}{\tau^m} \nabla_{\Gamma_h^m} \boldsymbol{u}_h^{m+1} : \nabla_{\Gamma_h^m} \boldsymbol{w}_h - \nabla_{\Gamma_h^m} \boldsymbol{\kappa}_h^{m+1} : \nabla_{\Gamma_h^m} \boldsymbol{w}_h$$

$$+ \sigma_h^{m+1} \nabla_{\Gamma_h^m} \cdot \boldsymbol{w}_h = r^m(\boldsymbol{w}_h),$$

$$\int_{\Gamma_h^m} \boldsymbol{\kappa}_h^{m+1} \cdot \boldsymbol{\psi}_h + \nabla_{\Gamma_h^m} \boldsymbol{u}_h^{m+1} : \nabla_{\Gamma_h^m} \boldsymbol{\psi}_h = - \int_{\Gamma_h^m} \nabla_{\Gamma_h^m} \boldsymbol{id}_h^m : \nabla_{\Gamma_h^m} \boldsymbol{\psi}_h,$$

$$\int_{\Gamma_h^m} \lambda_h \nabla_{\Gamma_h^m} \cdot \boldsymbol{u}_h^{m+1} = 0$$

where

$$r^m(\boldsymbol{w}_h) = \int_{\Gamma_h^m} \nabla_{\Gamma_h^m} \cdot \hat{\boldsymbol{\kappa}}_h^m \nabla_{\Gamma_h^m} \cdot \boldsymbol{w}_h + \frac{1}{2} |\hat{\boldsymbol{\kappa}}_h^m|^2 \nabla_{\Gamma_h^m} \cdot \boldsymbol{w}_h$$

$$- \boldsymbol{P}_h^m \nabla_{\Gamma_h^m} \hat{\boldsymbol{\kappa}}_h^m : \nabla_{\Gamma_h^m} \boldsymbol{w}_h - \nabla_{\Gamma_h^m} (\hat{\boldsymbol{\kappa}}_h^m)^T : \nabla_{\Gamma_h^m} \boldsymbol{w}_h.$$

Here, $\hat{\boldsymbol{\kappa}}_h^m \in V_h(\Gamma_h^m)$ is obtained from $\boldsymbol{\kappa}_h^m \in V_h(\Gamma_h^{m-1})$ by advancing the base functions while keeping the nodal values, and

$$(1) \qquad \Gamma_h^{m+1} = (\boldsymbol{id}_h^m + \tau^m \boldsymbol{u}_h^{m+1})(\Gamma_h^m).$$

The emerging linear algebra saddle point problem was solved with an UZAWA iteration where a direct method was used for the inner elliptic problem [2]. The code was implemented within ALBERTA [5].

Example (subproblem): Computations have been performed for the subproblem whose exact solution is given by

$$\boldsymbol{v} = \begin{pmatrix} 1 - x^4 \\ x(1-x^2)y \\ x(1-x^2)z \end{pmatrix}, \quad \sigma = \beta(10x^3 - 6x).$$

Reducing the grid spacing we obtain the expected orders of convergence:

step	h	L^2 error σ	eoc	H^1 error $\boldsymbol{v}$	eoc
0	0.75475	3.1606777	–	13.2176412	–
1	0.39775	1.7081632	0.9607	1.9160093	3.0150
2	0.20653	0.6769218	1.4123	0.3900714	2.4286
3	0.10433	0.1926953	1.8398	0.0741032	2.4320
4	0.05230	0.0498872	1.9569	0.0164731	2.1776
5	0.02617	0.0126008	1.9870	0.0039166	2.0744
6	0.01309	0.0031606	1.9957	0.0009576	2.0326
7	0.00654	0.0007911	1.9984	0.0002370	2.0148

Example (full problem): An ellipsoid was relaxed to a sphere and the presented flow was compared with the classical L^2 Willmore flow computed with the method of [4]. The local incompressiblity (or area preservation) constraint implies global area preservation. The numerical method computes a velocity field which weakly fulfils the constraint, but errors come in when moving the surface in the computed direction. For the suggested method (1) one expects an error in the global area of the order of the time step. Our findings agree with this, see the left figure below.
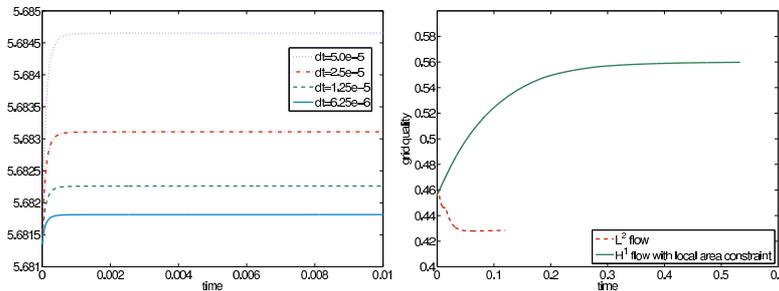
The right figure displays the grid quality for the H^1 flow with constraint in comparison with the classical L^2 flow.

References

[1] S. C. Brenner and L. R. Scott, *The mathematical theory of finite element methods*, third ed., Texts in Applied Mathematics, vol. 15, Springer, (2008).

[2] T. A. Davies, *Algorithm 832: Umfpack, an unsymmetric-pattern multifrontal method*, ACM Trans. Math. Software, 30 (2004), pp. 196–199.

[3] A. Demlow, *Higher-order finite element methods and pointwise error estimates for elliptic problems on surfaces*, SIAM J. Numer. Anal. 47 (2009), 805–827.

[4] G. Dziuk, *Computational parametric Willmore flow*, Numer. Math. 111 (2008), 55–80.

[5] A. Schmidt and K.G. Siebert, *Design of adaptive finite element software: The finite element toolbox ALBERTA*, Lecture notes in computational science and engineering, vol. 42, Springer (2005).

Nonconvex anisotropy and the bidomain model

Maurizio Paolini

(joint work with F. Pasquarelli, M. Bugatti)

Evolutions by gradient flow with nonconvex energies typically become ill-posed. As a motivating example consider the energy

$$(1) \qquad F(u) = \int_\Omega \Psi(u_x)\ dx$$

with Ω a bounded open interval in $\mathbb{R}$ and Ψ a double well potential with equal minima $\Psi(-1) = \Psi(1) = 0$ as shown in Figure 1 (left). The L^2 gradient flow associated to this energy reads

$$(2) \qquad \begin{cases} u_t = (\Psi'(u_x))_x \\ \text{some boundary condition at } \partial\Omega \end{cases}$$

which is a backward parabolic equation in the regions where $\Psi''(u_x)$ is negative and hence ill-posed.
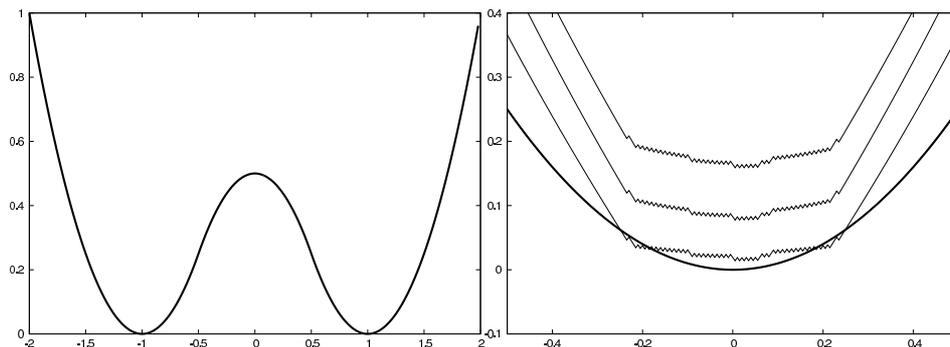
FIGURE 1. A typical double–well potential (left) and the corresponding evolution obtained with a finite difference space discretization of the gradient flow.

In order to recover a weak notion of solution it is customary to regularize equation (2) by adding small higher order terms or by applying some discretization procedure. If we e.g. discretize (2) in space by finite differences over a uniform grid we obtain the evolution shown in Figure 1 (right) starting from the thick curve. The evolution immediately produces wrinkles as small as the mesh size in the *backward parabolic* region of the curve which are then drawn up by the surrounding regular evolution. [5]

This is a common feature of most of the regularizations proposed for (2).

The bidomain model is a system of two reaction–diffusion equations in the unknowns u^i and u^e that reads as follows

$$(3) \qquad \begin{cases} \epsilon\partial_t(u^i - u^e) - \epsilon\mathrm{div}M^i u^i + \frac{1}{\epsilon}f(u^i - u^e) = 0 \\ \epsilon\partial_t(u^i - u^e) + \epsilon\mathrm{div}M^e u^e + \frac{1}{\epsilon}f(u^i - u^e) = 0 \end{cases}$$

in a 2D or 3D domain Ω, coupled with appropriate initial and boundary conditions. Here M^i, M^e are symmetric positive-definite matrices describing the underlying anisotropy, f is a cubic-like function, derivative of a double-well potential F which we assume to have two equal minima with zero value at ± 1 and the relaxation parameter $\epsilon > 0$ is small and dictates the thickness of the transition region of the transmembrane potential $u = u^i - u^e$.

This parabolic system is well-posed for any choice of the two symmetric positive-definite matrices [4].

By using matched asymptotics in [3] it was observed that the bidomain model exhibits a thin transition region that formally evolves (at first order) by anisotropic mean curvature [2], that is the velocity is given in vector form as

$$(4) \qquad\qquad \mathbf{V} = -\kappa_\varphi \mathbf{n}_\varphi$$

where the anisotropy φ^o is given by

$$(5) \qquad \varphi^o(\xi) = \sqrt{\frac{\alpha^i \alpha^e}{\alpha^i + \alpha^e}}, \qquad \alpha^i = \xi^T M^i \xi, \qquad \alpha^e = \xi^T M^e \xi.$$

Surprisingly φ^o becomes nonconvex for some choice of the matrices M^i and M^e. This is best illustrated in dimension 2 by chosing M^i, M^e diagonal with eigenvalues satisfying $\lambda_2^i = \rho\lambda_1^i$ and $\lambda_2^e = \frac{1}{\rho}\lambda_1^e$ with $\rho > 1$ a given *inverted* ratio. Figure 2 illustrates the situation for the two choices $\rho = 2$ (left) and $\rho = 10$ (right)

A Γ-convergence result for the stationary version of the bidomain model consistent with the asymptotic analysis has been proved in [1].

In the nonconvex case $\rho = 10$ we end up with a well-posed problem (the bidomain model) that is formally asymptotic to an ill-posed evolution (mean curvature flow with a nonconvex anisotropy). This fact deserves investigation, and motivates the numerical simulation of the bidomain model in a test case. We set $\Omega = (0, 1.2) \times (0, 1.2)$ with reflection condition along the coordinate axes and Dirichlet condition on the remaining boundary. The initial transmembrane potential $u = u^i - u^e$ has a transition region along a circle of radius 1 centered at the origin. We expect the transition region to shrink to a point in finite time during the evolution. Discretization is done with piecewise linear finite elements
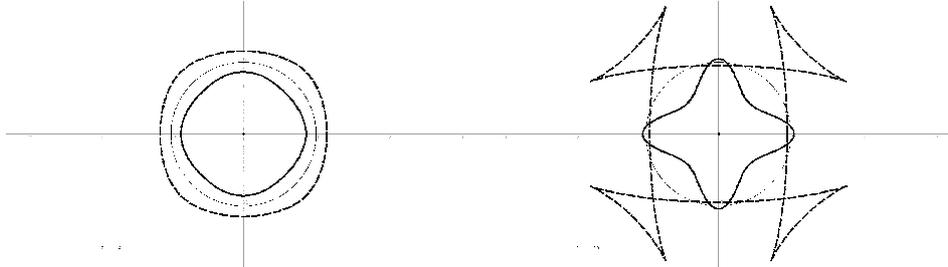
FIGURE 2. Plot of the Frank diagram ($\{\varphi^o \leq 1\}$, solid line) and its dual (Wulff shape, dashed line) for two choices of the inverted ratio: $\rho = 2$, eigenvalues 2 and 4 on the left and $\rho = 10$, eigenvalues 1 and 10 on the right.

in space and a coupling of an explicit Euler step for the first parabolic equation and a conjugate gradient solver at the next time step to recover u^i and u^e.

As shown in Figure 3 we observe after a very short time $t = 0.005$ the formation of wrinkles that later merge together and disappear leaving a transition layer homothetic to the Wulff shape with the swallowtails cutted off.
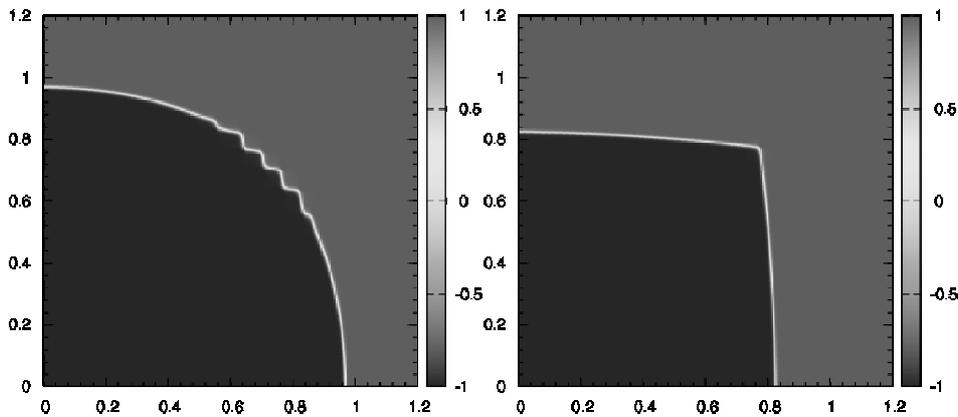
FIGURE 3. Numerical simulation of the bidomain model with $\rho = 10$ at times 0.005 (left) and 0.09 (right).

Such behaviour is quite interesting and deserves further investigation.

REFERENCES

[1] L. Ambrosio, P. Colli Franzone, G. Savaré, *On the asymptotic behaviour of anisotropic energies arising in the cardiac bidomain model*, Interfaces and Free Boundaries, **2** (2000), 213–266.

[2] G. Bellettini, M. Paolini, *Anisotropic motion by mean curvature in the context of Finsler geometry*, Hokkaido Math. J., **25** (1996), 537–566.

[3] G. Bellettini, P. Colli Franzone, M. Paolini, *Convergence of front propagation for anisotropic bistable reaction–diffusion equations*, Asymptotic Anal., **15** (1997), 325–358.

[4] P. Colli Franzone, G. Savaré, *Degenerate evolution systems modeling the cardiac electric field ad micro and macroscopic level*, Pubbl. IAN-CNR Pavia, **1007** (1996).

[5] F. Fierro, R. Goglione, M. Paolini *Numerical simulations of mean curvature flow in presence of a nonconvex anisotropy*, Math. Models Methods Appl. Sci., **4** (1998), 573–601.

Runge–Kutta time discretization of parabolic differential equations on evolving surfaces

CHRISTIAN LUBICH

(joint work with Gerhard Dziuk and Dhia Mansour)

The linear parabolic differential equation on a moving surface

$$\dot{u} + u\nabla_{\Gamma(t)} \cdot v - \Delta_{\Gamma(t)} u = f \quad \text{on } \Gamma(t)$$

is first discretized in space by evolving surface finite elements and then in time by an implicit Runge–Kutta method. The semi-discretization in space with piecewise linear surface finite elements, as studied in [1], leads to an ODE system for the coefficient vector $U(t)$ of the spatially discrete solution, of the form

$$\frac{d}{dt}(M(t)U(t)) + A(t)U(t) = F(t),$$

where $M(t)$ is the evolving mass matrix and $A(t)$ is the evolving stiffness matrix.

Following [2], we study implicit Runge–Kutta time discretizations for the spatially discretized problem, aiming for temporal stability uniformly in the space discretization and for higher-order bounds for the temporal error. The principal technical novelties are an abstract framework in which we can treat the spatially discretized equation, and a stability estimate in the natural time-dependent norms for Runge–Kutta methods that are algebraically stable and stiffly accurate, such as the Radau IIA methods. This permits us to analyse the convergence properties of such methods, leading to an order of convergence up to the classical order of the Runge–Kutta method. Numerical experiments with the Radau IIA time discretization illustrate the behaviour of the fully discrete method.

REFERENCES

[1] G. Dziuk and C.M. Elliott, *Finite elements on evolving surfaces*, IMA J. Numer. Anal. **27** (2007), 262–292.

[2] G. Dziuk, C. Lubich and D. Mansour, *Runge–Kutta time discretization of parabolic differential equations on evolving surfaces*, IMA J. Numer. Anal. (2011), doi:10.1093/imanum/drr017.

Parametric approximation of elastic flow for curves and curve networks

Robert Nürnberg

(joint work with John W. Barrett, Harald Garcke)

Let $(\Gamma(t))_{t \in [0,T]}$ be a family of closed curves in $\mathbb{R}^d$, $d \geq 2$, parameterized by $\vec{x}(\rho, t) : I \times [0,T] \to \mathbb{R}^d$, where $I := \mathbb{R}/\mathbb{Z}$. Introducing the arclength s of the curve, i.e. $\partial_s = |\vec{x}_\rho|^{-1} \partial_\rho$ on $\Gamma(t) \equiv \vec{x}(I, t)$, then

$$(1) \qquad \qquad \vec{\varkappa} := \vec{x}_{ss} \qquad \Rightarrow \qquad \vec{\varkappa} \,.\, \vec{x}_s = 0$$

denotes the usual curvature vector of Γ. For a given $\lambda \in \mathbb{R}$, we will consider the following elastic energy

$$(2) \qquad \qquad E_\lambda(\Gamma, \vec{\varkappa}) := \int_\Gamma \left[\tfrac{1}{2} |\vec{\varkappa}|^2 + \lambda \right] \mathrm{d}s \,,$$

where $\int_\Gamma f \, \mathrm{d}s := \int_I f \, |\vec{x}_\rho| \, \mathrm{d}\rho$ for $f : I \to \mathbb{R}$. In this talk we want to derive finite element approximations of the L^2-gradient flow of (2). This flow is of interest as a means to find stable critical points of (2), so called elasticae. Hence the L^2-gradient flow of (2), i.e.

$$(3) \qquad \qquad \vec{x}_t = -\vec{\nabla}_s^2 \, \vec{\varkappa} - \tfrac{1}{2} |\vec{\varkappa}|^2 \, \vec{\varkappa} + \lambda \, \vec{\varkappa} \,,$$

is commonly called elastic flow of curves. Here $\vec{\nabla}_s^2 \cdot := \vec{\nabla}_s (\vec{\nabla}_s \cdot)$ and $\vec{\nabla}_s \vec{\eta} := \vec{P} \vec{\eta}_s$ is the normal component of $\vec{\eta}_s$, where $\vec{P} := \vec{Id} - \vec{x}_s \otimes \vec{x}_s$ is the projection onto the part normal to Γ and $\vec{Id}$ is the identity operator/function on $\mathbb{R}^d$. The first error analysis for a numerical approximation of (3), including a stability result for a continuous-in-time semidiscrete finite element approximation, was recently presented in [9]. It is the aim of this talk to extend this stability analysis to an alternative finite element approximation, which retains some of the features of the schemes presented in previous work by the authors, see [1, 4, 5]; notably an equidistribution property.

On defining the test function space $\underline{V}_{0,\vec{\tau}} := \{\vec{\eta} \in \underline{V}_0 : \vec{\eta} \,.\, \vec{x}_s = 0\}$, where $\underline{V}_0 := H^1(I, \mathbb{R}^d)$ and $V_0 := H^1(I, \mathbb{R})$, the authors in [5] obtained the following weak formulation of (3) with $\vec{x}_t$ replaced by $\vec{P}\vec{x}_t$: Given $\Gamma(0) = \vec{x}(I, 0)$, with $\vec{x}(0) \in \underline{V}_0$, for all $t \in (0, T]$ find $\Gamma(t) = \vec{x}(I, t)$, where $\vec{x}(t) \in \underline{V}_0$, and $\vec{\varkappa}(t) \in \underline{V}_{0,\vec{\tau}}$ such that

$$(4a) \qquad \langle \vec{P} \, \vec{x}_t - \lambda \, \vec{\varkappa}, \vec{\chi} \rangle_\Gamma - \langle \vec{\nabla}_s \, \vec{\varkappa}, \vec{\nabla}_s \, \vec{\chi} \rangle_\Gamma - \tfrac{1}{2} \langle |\vec{\varkappa}|^2 \, \vec{x}_s, \vec{\chi}_s \rangle_\Gamma = 0 \quad \forall \, \vec{\chi} \in \underline{V}_{0,\vec{\tau}} \,,$$

$$(4b) \qquad \qquad \qquad \qquad \langle \vec{\varkappa}, \vec{\eta} \rangle_\Gamma + \langle \vec{x}_s, \vec{\eta}_s \rangle_\Gamma = 0 \quad \forall \, \vec{\eta} \in \underline{V}_0 \,.$$

Here $\langle \cdot, \cdot \rangle_\Gamma$ denotes the L^2-inner product on Γ; that is, $\langle u, v \rangle_\Gamma := \int_I u \,.\, v \, |\vec{x}_\rho| \, \mathrm{d}\rho$.

Unfortunately, for a finite element approximation based on the weak formulation (4a,b) it does not appear possible to prove a stability bound. Hence, on utilizing techniques from the formal calculus of PDE constrained optimization and ideas from [9], we derive a semidiscrete continuous-in-time finite element approximation that is stable and that satisfies an equidistribution property. To this end, we

consider the L^2-gradient flow of (2) for $\Gamma(t) = \vec{x}(I, t)$, with $\vec{x} \in \underline{V}_0$ and $\vec{\varkappa} \in \underline{V}_0$, subject to the side constraints

(5a) $$\langle \vec{\varkappa}, \vec{\eta} \rangle_\Gamma + \langle \vec{x}_s, \vec{\eta}_s \rangle_\Gamma = 0 \qquad \forall\, \vec{\eta} \in \underline{V}_0$$

(5b) and $$\langle \vec{\varkappa} \,.\, \vec{x}_s, \chi \rangle_\Gamma = 0 \qquad \forall\, \chi \in U_0\,,$$

where $U_0 := L^2(I, \mathbb{R})$. Here we should stress that the finite element discretization of the constraints (5a,b), building on the ideas published in the series of papers [1, 2, 4, 5, 6], will lead to an induced tangential motion that gives rise to an equidistribution property in the semidiscrete setting. Of course, on the continuous level the side constraint (5b) is redundant, recall (1). Introducing the Lagrange multipliers $\vec{y} \in \underline{V}_0$ and $z \in U_0$ for (5a,b), we define the Lagrangian

$$\mathcal{L}(\vec{x}, \vec{\varkappa}, \vec{y}, z) := \tfrac{1}{2}\, \langle \vec{\varkappa}, \vec{\varkappa} \rangle_\Gamma + \lambda\, |\Gamma| - \langle \vec{\varkappa}, \vec{y} \rangle_\Gamma - \langle \vec{x}_s, \vec{y}_s \rangle_\Gamma + \langle \vec{\varkappa} \,.\, \vec{x}_s, z \rangle_\Gamma\,,$$

where $|\Gamma| := \langle 1, 1 \rangle_\Gamma$ is the length of Γ. Hence we obtain, on taking variations $[\frac{\delta}{\delta \vec{x}} \mathcal{L}](\vec{\chi})$, $[\frac{\delta}{\delta \vec{\varkappa}} \mathcal{L}](\vec{\xi})$, $[\frac{\delta}{\delta \vec{y}} \mathcal{L}](\vec{\eta})$ and $[\frac{\delta}{\delta z} \mathcal{L}](\chi)$, that the direction of steepest descent of E_λ under the constraints (5a,b) is given by $-[\frac{\delta}{\delta \vec{x}} \mathcal{L}](\vec{\chi})$, with the remaining variations of $\mathcal{L}$ set to zero. In particular, we obtain the gradient flow

(6a) $\langle \vec{P}\, \vec{x}_t, \vec{\chi} \rangle_\Gamma = \langle \vec{\nabla}_s\, \vec{y}, \vec{\nabla}_s\, \vec{\chi} \rangle_\Gamma - \tfrac{1}{2} \langle (|\vec{\varkappa}|^2 - 2\,\vec{\varkappa} \,.\, \vec{y} + 2\,\lambda)\, \vec{x}_s, \vec{\chi}_s \rangle_\Gamma - \langle z\, \vec{\varkappa}, \vec{\chi}_s \rangle_\Gamma\,,$

(6b) $\langle \vec{\varkappa} + z\, \vec{x}_s - \vec{y}, \vec{\xi} \rangle_\Gamma = 0\,,$

(6c) $\langle \vec{\varkappa}, \vec{\eta} \rangle_\Gamma + \langle \vec{x}_s, \vec{\eta}_s \rangle_\Gamma = 0\,,$

(6d) $\langle \vec{\varkappa} \,.\, \vec{x}_s, \chi \rangle_\Gamma = 0\,;$

for all $\vec{\chi}, \vec{\xi} \in \underline{V}_0$, $\eta, \chi \in U_0$. It follows from (6b,d) that $\vec{P}\, \vec{y} = \vec{\varkappa}$ and $z = \vec{y} \,.\, \vec{x}_s$. Hence the normal part of the Lagrange multiplier $\vec{y}$ agrees with the curvature vector, but in addition it may have a nonzero tangential component z. Overall our formal weak formulation of the L^2-gradient flow for (2) subject to (5a,b) can now be formulated as: Given $\Gamma(0) = \vec{x}(I, 0)$, with $\vec{x}(0) \in \underline{V}_0$, for all $t \in (0, T]$ find $\Gamma(t) = \vec{x}(I, t)$, where $\vec{x}(t) \in \underline{V}_0$, and $\vec{y}(t) \in \underline{V}_0$ such that

(7a) $\langle \vec{P}\, \vec{x}_t, \vec{\chi} \rangle_\Gamma = \langle \vec{\nabla}_s\, \vec{y}, \vec{\nabla}_s\, \vec{\chi} \rangle_\Gamma + \tfrac{1}{2} \langle (|\vec{P}\, \vec{y}|^2 - 2\,\lambda)\, \vec{x}_s, \vec{\chi}_s \rangle_\Gamma - \langle (\vec{y} \,.\, \vec{x}_s)\, \vec{P}\, \vec{y}, \vec{\chi}_s \rangle_\Gamma\,,$

(7b) $\langle \vec{P}\, \vec{y}, \vec{\eta} \rangle_\Gamma + \langle \vec{x}_s, \vec{\eta}_s \rangle_\Gamma = 0\,;$

for all $\vec{\chi}, \vec{\eta} \in \underline{V}_0$. On noting that $\langle \vec{\nabla}_s\, \vec{y}, \vec{\nabla}_s\, \vec{\chi} \rangle_\Gamma - \langle (\vec{y} \,.\, \vec{x}_s)\, \vec{P}\, \vec{y}, \vec{\chi}_s \rangle_\Gamma = \langle \vec{\nabla}_s\, \vec{\varkappa}, \vec{\nabla}_s\, \vec{\chi} \rangle_\Gamma$ we see that (7a,b) is independent of the tangential component $\vec{y} \,.\, \vec{x}_s$. Moreover, in common with similar formulations of general geometric evolution equations in the series of papers [1, 2, 3, 5], the tangential part $(\vec{Id} - \vec{P})\, \vec{x}_t$, of the velocity vector $\vec{x}_t$ is not prescribed in (7a,b). Hence there does not exist a unique solution to (7a,b). Under spatial discretization, the tangential part of the discrete approximation to $\vec{x}_t$ will be intrinsically fixed, and this choice will lead to an equidistribution property.

Replacing $\mathcal{L}$ with the discrete Lagrangian $\mathcal{L}^h(\vec{X}^h, \vec{\kappa}^h, \vec{Y}^h, Z^h) := \tfrac{1}{2} \langle \vec{\kappa}^h, \vec{\kappa}^h \rangle^h_{\Gamma^h} + \lambda\, |\Gamma^h| - \langle \vec{\kappa}^h, \vec{Y}^h \rangle^h_{\Gamma^h} - \langle \vec{X}^h_s, \vec{Y}^h_s \rangle_{\Gamma^h} + \langle \vec{\kappa}^h \,.\, \vec{X}^h_s, Z^h \rangle^h_{\Gamma^h}$, where $\vec{X}^h, \vec{\kappa}^h, \vec{Y}^h \in \underline{V}^h_0 := \{\vec{\chi} \in C(I, \mathbb{R}^d) : \vec{\chi}\,|_{I_j}$ is linear $\forall\, j = 1 \to J\} =: [V^h_0]^d \subset H^1(I, \mathbb{R}^d)$ and $Z^h \in V^h_0$, it is possible to repeat the above procedure on the discrete level in order to obtain
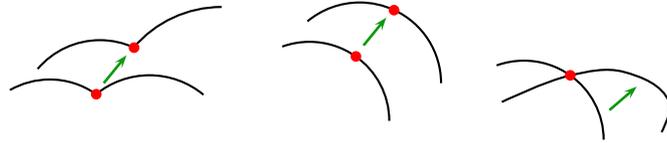
FIGURE 1. Different types of junctions (left to right): a moving C^0-junction, a moving C^1-junction and a stationary C^2-nonlinear spline junction.

the desired semidiscrete finite element approximation. An extension to anisotropic curve energies is also possible, see [7] for details.

These ideas can be extended to the case of open curves, where suitable boundary conditions have to be applied at the two endpoints of the curve. Of interest are clamped and Navier boundary conditions. Finally, we also consider the elastic flow for curve networks. Here meaningful and relevant conditions at junction points need to be derived and suitably discretized. Examples for junction points are C^0-junctions, C^1-junctions and C^2-nonlinear spline junctions; see Figure 1. We refer to [8] for more details on the approximation of the elastic flow of curve networks. The numerical results presented in this talk demonstrate the practicality of the introduced finite element approximations.

REFERENCES

[1] J. W. Barrett, H. Garcke, and R. Nürnberg. *A parametric finite element method for fourth order geometric evolution equations*, J. Comput. Phys. **222** (2007), 441–462.

[2] J. W. Barrett, H. Garcke, and R. Nürnberg. *On the variational approximation of combined second and fourth order geometric evolution equations*, SIAM J. Sci. Comput. **29** (2007), 1006–1041.

[3] J. W. Barrett, H. Garcke, and R. Nürnberg. *Numerical approximation of anisotropic geometric evolution equations in the plane*, IMA J. Numer. Anal. **28** (2008), 292–330.

[4] J. W. Barrett, H. Garcke, and R. Nürnberg. *Parametric approximation of Willmore flow and related geometric evolution equations*, SIAM J. Sci. Comput. **31** (2008), 225–253.

[5] J. W. Barrett, H. Garcke, and R. Nürnberg. *Numerical approximation of gradient flows for closed curves in $\mathbb{R}^d$*, IMA J. Numer. Anal. **30** (2010), 4–60.

[6] J. W. Barrett, H. Garcke, and R. Nürnberg. *The approximation of planar curve evolutions by stable fully implicit finite element schemes that equidistribute*, Numer. Methods Partial Differential Equations **27** (2011), 1–30.

[7] J. W. Barrett, H. Garcke, and R. Nürnberg. *Parametric approximation of isotropic and anisotropic elastic flow for closed and open curves*, Numer. Math. (2011), `doi:10.1007/s00211-011-0416-x`.

[8] J. W. Barrett, H. Garcke, and R. Nürnberg. *Elastic flow with junctions: Variational approximation and applications to nonlinear splines*, Preprint No. 30/2011, University Regensburg, Germany (2011).

[9] K. Deckelnick and G. Dziuk. *Error analysis for the elastic flow of parametrized curves*, Math. Comp. **78** (2009), 645–671.

Computation of Ricci curvature

Hans Fritz

(joint work with Gerhard Dziuk)

In 1982 Ricci flow was introduced by Richard Hamilton, and since then a well-developed theory of Ricci flow has been established. In contrast, the hitherto existing numerical studies of Ricci flow are still restricted to special cases, e.g. [1], [2], [3], [4]. One reason for this is that, up to now, there is no general formulation of Ricci curvature, which is open for a consistent finite element approach. This situation remains unsatisfactory even more, since there has been significant progress in the computation of geometric flows like mean curvature flow and Willmore flow [5], [6]. Studying these flows, a finite element method on triangulated hypersurfaces [7], [8] has emerged as a particularly adequate ansatz for developing numerical algorithms for geometric PDEs. Within the scope of this method it is possible to define discrete curvatures on polyhedral surfaces by discretizing weak formulations and, moreover, to prove approximation results [9].

Following this approach we present a definition of discrete Ricci curvature on triangulated hypersurfaces of arbitrary dimension n, which is based on a weak formulation and which does not make use of special assumptions of symmetries. Starting with a formula first proved by Yano, see [10], we get a weak formulation of Ricci curvature on isometrically embedded hypersurfaces $\Gamma \subset \mathbb{R}^{n+1}$ only containing tangential gradients. A discretization of this formulation leads naturally to the definition of discrete Ricci curvature on triangulated hypersurfaces, this means that we define discrete Ricci curvature as the $L^2(\Gamma)$-projection of a discretized curvature functional. With an appropriate choice of a discrete tangential projection the definition depends solely on quantities of the discrete surface. However, linear convergence against the Ricci curvature of Γ in the $L^2(\Gamma)$-norm can be proved only in the case $n \leq 3$ and for an at least quadratic approximation Γ_{h2} of Γ with isoparametric Lagrange finite elements. Using a discrete version of the smoothing operator $(\mathbb{1} - \epsilon\Delta_\Gamma)^{-1} : W^{-1}(\Gamma) \to W^{1,2}(\Gamma)$, it is also possible to reconstruct Ricci curvature on a piecewise linear triangulation Γ_{h1}, see also [11].

In the following we assume $\Gamma \subset \mathbb{R}^{n+1}$ to be a smooth, closed, orientable and connected hypersurface and $\Gamma_{h1} = \bigcup_{T \in \mathcal{T}_{h1}} T$ to be an admissible, quasi-uniform triangulation with a maximal diameter h of the simplices $T \in \mathcal{T}_{h1}$ and with vertices sitting on Γ. There is a strip Γ_δ of width δ about Γ such that the projection

$$a(x) = x - d(x)\nu(x) \ \in \Gamma,$$

is unique $\forall x \in \Gamma_\delta$, where d is the oriented distance function of Γ, and ν is the unit outward normal. We suppose that $\Gamma_{h1} \subset \Gamma_\delta$, and in addition that $a : \Gamma_{h1} \to \Gamma$ is a bijective map, see [5] for details. The lift of a function f onto Γ is $f^l := f \circ a^{-1}$. The Lagrange interpolation of second order of $a_{|\Gamma_{h1}}$ is denoted by a_2, and the isoparametric hypersurface of second order is defined by $\Gamma_{h2} := \left\{ a_2(x) \in \mathbb{R}^{n+1} | \ x \in \Gamma_{h1} \right\}$. The finite element spaces on Γ_{h1} and Γ_{h2}

respectively are

$$S_{h1} := \left\{ \, \chi \in C^0(\Gamma_{h1}) \mid \chi_{|T} \in \mathbb{P}_1 \; \forall T \in \mathcal{T}_{h1} \, \right\},$$
$$S_{h2} := \left\{ \, \tilde{\chi} \in C^0(\Gamma_{h2}) \mid \tilde{\chi} \circ a_2 = \chi \text{ for some } \chi \in S_{h1} \, \right\}.$$

With the projection $P = \mathbb{1} - \nu \otimes \nu$ the Ricci curvature ric of Γ in the basis of the ambient space $\mathbb{R}^{n+1}$ is denoted by $(Ric_\gamma)_\alpha := ric(Pe_\gamma, Pe_\alpha)$ for $\alpha, \gamma = 1, \ldots, n+1$.

Lemma 1. *Let $P_{h2} \in (S_{h2})^{(n+1)\times(n+1)}$ be the solution of*

$$\int_{\Gamma_{h2}} I\left(P_{h2} : \psi\right) = \sum_{T \in \mathcal{T}_{h2}} \int_T I_{|T}\left(\widetilde{P}_{h2|T} : \psi_{|T}\right), \quad \forall \psi \in (S_{h2})^{(n+1)\times(n+1)},$$

where I is the linear Lagrange interpolant on Γ_{h2}, and $\widetilde{P}_{h2} = \mathbb{1} - \nu_{h2} \otimes \nu_{h2}$ is the projection on the tangent space of Γ_{h2}. For $n \leq 3$ the lift P_{h2}^l onto Γ approximates the projection P,

$$\|P - P_{h2}^l\|_{L^\infty(\Gamma)} \leq C(\Gamma)h^2.$$

Theorem 1. *Let $Ric_{h\gamma} \in (S_{h2})^{n+1}$, $\gamma = 1, \ldots, n+1$, be the solution of*

$$\int_{\Gamma_{h2}} Ric_{h\gamma} \cdot \psi = \sum_{\alpha,\beta=1}^{n+1} \int_{\Gamma_{h2}} \left(\underline{D}_\alpha P_{h2\gamma}^\alpha \underline{D}_\beta I(P_{h2}\psi)^\beta - \underline{D}_\alpha P_{h2\gamma}^\beta \underline{D}_\beta I(P_{h2}\psi)^\alpha\right),$$

$\forall \psi \in (S_{h2})^{n+1}$, where I is the linear Lagrange interpolant, and $\underline{D}_\alpha(\cdot)$ are the components of the tangential gradient on Γ_{h2}. Then for $n \leq 3$ the following estimates hold,

$$\|Ric_\gamma - Ric_{h\gamma}^l\|_{L^2(\Gamma)} \leq C(\Gamma)h, \quad \gamma = 1, \ldots, n+1.$$

Lemma 2. *Let $P_{h1} \in (S_{h1})^{(n+1)\times(n+1)}$ be the solution of*

$$\int_{\Gamma_{h1}} I\left(P_{h1} : \psi\right) = \int_{\Gamma_{h1}} \widetilde{P}_{h1} : \psi, \quad \forall \psi \in (S_{h1})^{(n+1)\times(n+1)},$$

where I is the linear Lagrange interpolant on Γ_{h1}, and $\widetilde{P}_{h1} = \mathbb{1} - \nu_{h1} \otimes \nu_{h1}$ is the projection on the tangent space of Γ_{h1}. For $n \leq 3$ the lift P_{h1}^l onto Γ approximates the projection P,

$$\|P - P_{h1}^l\|_{L^\infty(\Gamma)} \leq C(\Gamma)h.$$

Theorem 2. *Let $Ric_{h\gamma}^\epsilon \in (S_{h1})^{n+1}$, $\gamma = 1, \ldots, n+1$, be the solution of*

$$\int_{\Gamma_{h1}} Ric_{h\gamma}^\epsilon \cdot \psi + \epsilon \nabla_{\Gamma_{h1}} Ric_{h\gamma}^\epsilon : \nabla_{\Gamma_{h1}} \psi$$
$$= \sum_{\alpha,\beta=1}^{n+1} \int_{\Gamma_{h1}} \left(\underline{D}_\alpha P_{h1\gamma}^\alpha \underline{D}_\beta I(P_{h1}\psi)^\beta - \underline{D}_\alpha P_{h1\gamma}^\beta \underline{D}_\beta I(P_{h1}\psi)^\alpha\right),$$

$\forall \psi \in (S_{h1})^{n+1}$, where I is the linear Lagrange interpolant, and $\underline{D}_\alpha(\cdot)$ are the components of the tangential gradient on Γ_{h1}. Then for $n \leq 3$ and $\epsilon = h^{\frac{2}{3}}$ the

following estimates hold,

$$\|Ric_\gamma - Ric_{h\gamma}^{\epsilon l}\|_{L^2(\Gamma)} \le C(\Gamma)h^{\frac{2}{3}}, \quad \gamma = 1, \ldots, n+1,$$

$$\|\nabla_\Gamma(Ric_\gamma - Ric_{h\gamma}^{\epsilon l})\|_{L^2(\Gamma)} \le C(\Gamma)h^{\frac{1}{3}}, \quad \gamma = 1, \ldots, n+1.$$

Numerical tests for two and three dimensional hypersurfaces of different genus, which were performed within the finite element toolbox ALBERTA [12], confirm our theoretical results.

Since Ricci flow is an intrinsic flow, it is necessary for numerical simulations to generalize the above definitions to the case, when the Riemannian metric is not induced by an embedding in an Euclidean space. We discuss a possibility to do this if the n-dimensional Riemannian manifold (Γ, g) is embedded as a differentiable manifold in $\mathbb{R}^{n+1}$. Then an extension G of the Riemannian metric g to the open strip $\Gamma_\delta \subset \mathbb{R}^{n+1}$ can be defined such that (Γ, g) is a Riemannian submanifold of the Riemannian manifold (Γ_δ, G), this means that $g = G_{|T\Gamma \times T\Gamma}$. Because Γ_δ has a trivial atlas, which only contains the identity map on Γ_δ, it is possible to avoid local parametrizations by using the extension G for computations instead of the Riemannian metric g itself. Hence, the problem can be handled within the scope of a surface finite element method.

REFERENCES

[1] D. Garfinkle and J. Isenberg, *Numerical studies of the behavior of Ricci flow*, in Geometric Evolution Equations, volume 367 of Contemporary Mathematics, AMS (2005).

[2] D. Garfinkle and J. Isenberg, *The modeling of degenerate neck pinch singularities in Ricci flow by Bryant solitons*, J. Math. Phys. 49, 073505 (2008).

[3] J. H. Rubinstein and R. Sinclair, *Visualizing Ricci flow of manifolds of revolution*, Experiment. Math. Volume 14, Issue 3 (2005), 285–298.

[4] M. Jin, J. Kim, F. Luo and X. Gu, *Discrete Surface Ricci Flow*, IEEE Trans. Visualization and Computer Graphics, vol. 14, no. 5 (2008), 1030–1043.

[5] K. Deckelnick, G. Dziuk and C. M. Elliott, *Computation of geometric partial differential equations and mean curvature flow*, Acta Numerica (2005), 139–232.

[6] G. Dziuk, *Computational parametric Willmore flow*, Numer. Math. No. 111 (2008), 55–80.

[7] G. Dziuk, *Finite elements for the Beltrami operator on arbitrary surfaces*, In S. Hildebrandt and R. Leis, editors, Partial Differential Equations & Calculus of Variations, volume 1357 of Lecture Notes in Math., Springer (1988), 142–155.

[8] A. Demlow, *Higher-order finite element methods and pointwise error estimates for elliptic problems on surfaces*, SIAM J. Numer. Anal. 47 (2009), 805–827.

[9] C.-J. Heine, *Isoparametric finite element approximation of curvature on hypersurfaces*, Preprint, Fakultät für Mathematik und Physik, Universität Freiburg, Nr. 26 (2004).

[10] K. Yano, *On Harmonic and Killing Vector Fields*, The Annals of Mathematics, Second Series, Vol. 55, No. 1 (1952), 38–45.

[11] C.-J. Heine, *Curvature reconstruction with linear finite elements*, Unpublished (2009).

[12] A. Schmidt and K. G. Siebert, *Design of Adaptive Finite Element Software*, Springer, Lecture Notes in Computational Science and Engineering 42 (2005).

Threshold dynamics for arbitrary surface tensions

Selim Esedoglu

(joint work with Felix Otto)

In [4], Merriman, Bence, and Osher proposed an interesting algorithm for generating the motion by mean curvature of an interface. Given an initial set $\Sigma^0 \subset \mathbb{R}^3$ the boundary $\partial\Sigma^0$ of which is to be evolved by mean curvature motion, along with a time step size δt, it generates a discrete in time approximation $\{\Sigma^k\}$ to the flow by alternating the following two very simple operations:

(1) <u>Convolution</u>: Form the diffused out function $u(x)$:

$$u^k(x) = G_{\delta t} * \mathbf{1}_{\Sigma^k}(x) \text{ where } G_t = \frac{1}{(4\pi t)^{3/2}} e^{-|x|^2/4t}$$

(2) <u>Thresholding</u>: Define the approximation Σ^{k+1} to the flow at time $t = k\delta t$ according to:

$$\Sigma^{k+1} = \left\{ x \; : \; u^k(x) \geq \frac{1}{2} \right\}.$$

One of the greatest benefits of this algorithm is its unconditional stability: The time step size δt is restricted only by accuracy considerations. Moreover, each step of the algorithm can be implemented very efficiently: On a uniform grid, the convolution step can be accomplished in $O(n \log n)$ operations, where n is the total number of grid points, and the thresholding step is just pointwise and trivial.

In their original paper [4], the authors showed how their algorithm can also be adapted to the case of *multi-phase* curvature flow in certain special cases. Here, the problem is to simulate L^2 gradient descent for the energy

$$(1) \qquad\qquad E(\Sigma_1, \ldots, \Sigma_N) = \sum_{j=1}^{N} \mathrm{Per}(\Sigma_j)$$

where the sets Σ_j satisfy

$$\Sigma_i \cap \Sigma_j = (\partial\Sigma_i) \cap (\partial\Sigma_j) \text{ for all } i \neq j, \text{ and } \bigcup_{j=1}^{N} \Sigma_j = D$$

and D is a domain in $\mathbb{R}^n$. The sets Σ_j thus constitute a partitioning of D, filling it up, and intersecting only at their boundaries. Gradient descent for this energy leads to the following dynamics at smooth points along an interface $\Gamma_{i,j} = (\partial\Sigma_i) \cap (\partial\Sigma_j)$ separating the two phases Σ_i and Σ_j:

$$(2) \qquad\qquad v_n(x) = \kappa(x)$$

where $\kappa(x)$ denotes the curvature at $x \in \Gamma_{i,j}$ and $v_n(x)$ denotes the normal speed of the interface at the same point. In addition, natural boundary conditions known as *Herring angle conditions* [2] hold along triple curves where three interfaces $\Gamma_{i,j}$, $\Gamma_{j,k}$, and $\Gamma_{k,i}$ meet:

$$(3) \qquad\qquad n_{i,j} \cdot n_{j,k} = n_{j,k} \cdot n_{k,i} = n_{k,i} \cdot n_{i,j} = -\frac{1}{2}$$

where $n_{i,j}$ denotes the unit normal along $\Gamma_{i,j}$.

Dynamics given in (2) & (3) arises in certain well-known models of grain boundary motion in polycrystals [5]. The algorithm that was given in [4] for this flow is as follows: Given the initial partition $(\Sigma_1^0, \ldots, \Sigma_N^0)$ of the domain D and a time step size δt, generate the discrete in time approximation $(\Sigma_1^k, \ldots, \Sigma_N^k)$ at time $t = k\delta t$ by alternating the following two steps:

(1) <u>Convolution:</u> Form the functions

$$u_j^k(x) = G_{\delta t} * \mathbf{1}_{\Sigma_j^k}.$$

(2) <u>Redistribution:</u>

$$\Sigma_j^{k+1} = \left\{ x \,:\, u_j^k(x) \geq \max_{i \neq j} u_i^k(x) \right\}.$$

In the materials science literature, energy (1) appears as a special case of the following more general model:

$$(4) \qquad E(\Sigma_1, \ldots, \Sigma_N) = \sum_{j=1}^{N} \sigma_{i,j} \mathrm{Area}(\Gamma_{i,j})$$

where the weights (i.e. the *surface tensions*) $\sigma_{i,j} > 0$ are arbitrary except for satisfying a *triangle inequality*, which turns out to be necessary for well-posedness:

$$\sigma_{i,j} + \sigma_{j,k} \geq \sigma_{i,k} \text{ for any distinct } i, j, \text{ and } k.$$

The relevant dynamics is now:

$$(5) \qquad v_n(x) = \sigma_{i,j}\kappa(x)$$

at smooth points x along the interface $\Gamma_{i,j}$ between Σ_i and Σ_j, together with the angle condition

$$(6) \qquad \sigma_{i,j}n_{i,j} + \sigma_{j,k}n_{j,k} + \sigma_{k,i}n_{k,i} = 0$$

that needs to hold along any triple curves where $\Gamma_{i,j}$, $\Gamma_{j,k}$, and $\Gamma_{k,i}$ might meet. The greater generality of model (5) & (6) as compared to the simpler (2) & (3) is required to capture certain important phenomena, such as grain boundary character distribution [1].

Generalizing the threshold dynamics algorithm for the special (i.e. equal surface tension, $\sigma_{i,j} = 1$) case of model (2) & (3) to the more general model (5) & (6) has been of interest for a long time, starting with the original paper [4]. Indeed, attempts in this direction were already made in [4] and later in [3] by modifying the redistribution step of the algorithm, e.g. by weighting the terms $u_i^k(x)$ by appropriate constants, so that the desired angles (6) at triple junctions are attained. However, the choice of these constants suggested in previous works were incorrect. Consequently, how to properly choose them had remained unknown. It should be pointed out that an alternative, correct algorithm for (5) & (6) was given in [6], but required modifying the redistribution step of the original algorithm to be spatially varying, deviating somewhat from the simplicity of the original scheme.

In joint work with Felix Otto, we determine how to correctly modify the redistribution step of the original multi-phase threshold dynamics algorithm by a very simple generalization (that incorporates constant weights the choice of which depend on the surface tensions $\sigma_{i,j}$) so that the desired angle conditions (6) and the normal speeds (5) are attained.

REFERENCES

[1] D. Kinderlehrer, I. Livshitz, G. S. Rohrer, S. Taasan, P. Yu, *Mesoscale simulation of the evolution of the grain boundary character distribution*, Recrystallization and Grain Growth. Parts 1 and 2. (2004), 1063–1068.
[2] C. Herring, *Surface tension as a motivation for sintering*, McGraw Hill (1951), 143–179.
[3] P. Mascarenhas, *Diffusion generated motion by mean curvature*, UCLA CAM Report 92–33 (1992).
[4] B. Merriman, J. K. Bence, S. Osher, *Motion of multiple junctions: a level set approach*, J. Comp. Phys. **112**:2 (1994), 334–363.
[5] W. W. Mullins, *Two dimensional motion of idealized grain boundaries*, J. Appl. Phys. **27** (1956), 900–904.
[6] S. J. Ruuth, *A diffusion generated approach to multiphase motion*, J. Comp. Phys. **145** (1998), 166–192.

Reporter: Ralf Kornhuber

Participants

Prof. Dr. Helmut Abels
Fakultät für Mathematik
Universität Regensburg
Universitätsstr. 31
93053 Regensburg

Prof. Dr. Sören Bartels
Institut für Numerische Simulation
Universität Bonn
Wegelerstr. 6
53115 Bonn

Prof. Dr. Andrea Bonito
Department of Mathematics
Texas A & M University
College Station , TX 77843-3368
USA

Prof. Dr. Klaus Deckelnick
Institut für Analysis u. Numerik
Otto-von-Guericke-Universität
Magdeburg
Universitätsplatz 2
39106 Magdeburg

Prof. Dr. Wolfgang Dreyer
Weierstraß-Institut für
Angewandte Analysis und Stochastik
Mohrenstr. 39
10117 Berlin

Prof. Dr. Gerhard Dziuk
Abteilung für Angewandte Mathematik
Universität Freiburg
Hermann-Herder-Str. 10
79104 Freiburg

Prof. Dr. Klaus Ecker
FB Mathematik & Informatik
Freie Universität Berlin
Arnimallee 3
14195 Berlin

Prof. Dr. Charles M. Elliott
Mathematics Institute
University of Warwick
Gibbet Hill Road
GB-Coventry CV4 7AL

Prof. Dr. Selim Esedoglu
Department of Mathematics
University of Michigan
530 Church Street
Ann Arbor , MI 48109-1043
USA

Hans Fritz
Abteilung f. Angewandte Mathematik
Universität Freiburg
Eckerstr. 1
79104 Freiburg

Prof. Dr. Harald Garcke
NWF I - Mathematik
Universität Regensburg
93040 Regensburg

Dr. Romain Gicquaud
Departement de Mathematiques
Faculte des Sciences
Universite de Tours
Parc de Grandmont
F-37200 Tours

Prof. Dr. Mi-Ho Giga
Graduate School of
Mathematical Sciences
University of Tokyo
3-8-1 Komaba, Meguro-ku
Tokyo 153-8914
JAPAN

Prof. Dr. Yoshikazu Giga
Department of Mathematics
Graduate School of Math. Sciences
The University of Tokyo, Komaba Campus
7-3-1 Hongo, Bunkyo-ku
Tokyo 113-0033
JAPAN

Carsten Gräser
Fachbereich Mathematik & Informatik
Freie Universität Berlin
Arnimallee 6
14195 Berlin

Hanne Hardering
Fachbereich Mathematik & Informatik
Freie Universität Berlin
Arnimallee 6
14195 Berlin

Dr. Claus-Justus Heine
Fachbereich Mathematik
Universität Stuttgart
Pfaffenwaldring 57
70569 Stuttgart

Prof. Dr. Michael Holst
Department of Mathematics
University of California, San Diego
9500 Gilman Drive
La Jolla , CA 92093-0112
USA

Prof. Dr. Gerhard Huisken
MPI für Gravitationsphysik
Albert-Einstein-Institut
Am Mühlenberg 1
14476 Golm

Prof. Dr. James Isenberg
Department of Mathematics
University of Oregon
Eugene , OR 97403-5203
USA

Prof. Dr. Ralf Kornhuber
Institut für Mathematik
Freie Universität Berlin
Arnimallee 6
14195 Berlin

Prof. Dr. Dietmar Kröner
Abteilung für Angewandte Mathematik
Universität Freiburg
Hermann-Herder-Str. 10
79104 Freiburg

Andrew Lam
Mathematics Institute
University of Warwick
Gibbet Hill Road
GB-Coventry CV4 7AL

Prof. Dr. Philippe G. LeFloch
Laboratoire Jacques-Louis Lions
Universite Paris 6
4, Place Jussieu
F-75252 Paris Cedex 05

Prof. Dr. Christian Lubich
Mathematisches Institut
Universität Tübingen
Auf der Morgenstelle 10
72076 Tübingen

Dr. Thomas Maerz
Mathematical Institute
Oxford University
24-29 St. Giles
GB-Oxford OX1 3LB

Prof. Dr. Matteo Novaga
Dipartimento di Matematica
Universita di Padova
Via Trieste, 63
I-35121 Padova

Dr. Robert Nürnberg
Department of Mathematics
Imperial College London
Huxley Building
GB-London SW7 2AZ

Dr. Michael Oevermann
Fachbereich Mathematik & Informatik
Freie Universität Berlin
Arnimallee 6
14195 Berlin

Prof. Dr. Maurizio Paolini
Dipartimento di Matematica e Fisica
Universita Cattolica del Sacro Cuore
di Brescia
Via Musei 41
I-25121 Brescia

Prof. Dr. Konrad Polthier
Institut für Mathematik
Freie Universität Berlin
Arnimallee 6
14195 Berlin

Prof. Dr. Paola Pozzi
Fachbereich Mathematik
Universität Duisburg-Essen
Lotharstr. 65
47057 Duisburg

Tom Ranner
Mathematics Institute
University of Warwick
Gibbet Hill Road
GB-Coventry CV4 7AL

Prof. Dr. Arnold Reusken
Institut für Geometrie und
Praktische Mathematik
RWTH Aachen
Templergraben 55
52061 Aachen

Dr. Oliver Rinne
Albert-Einstein-Institut
MPI für Gravitationsphysik
Am Mühlenberg 1
14476 Golm

Prof. Dr. Matthias Röger
Fachbereich Mathematik
Technische Universität Dortmund
Vogelpothsweg 87
44227 Dortmund

Prof. Dr. Martin Rumpf
Hausdorff Center for Mathematics
Institute for Numerical Simulation
Endenicher Allee 60
53115 Bonn

Prof. Dr. Oliver Sander
Fachbereich Mathematik & Informatik
Freie Universität Berlin
Arnimallee 6
14195 Berlin

Prof. Dr. James A. Sethian
Department of Mathematics
University of California
Berkeley CA 94720-3840
USA

Jan Steinhilber
Hermann-Herder-Str. 10
79104 Freiburg

Dr. Björn Stinner
Mathematics Institute
University of Warwick
Gibbet Hill Road
GB-Coventry CV4 7AL

Prof. Dr. Endre Süli
Mathematical Institute
Oxford University
24-29 St. Giles
GB-Oxford OX1 3LB

Prof. Dr. Lutz Tobiska
Institut für Analysis und Numerik
Otto-von-Guericke-Universität
Magdeburg
Postfach 4120
39016 Magdeburg

Orestis Vantzos
Hausdorff Center for Mathematics
Institute for Numerical Simulation
Endenicher Allee 60
53115 Bonn

Dr. Chandrashekar Venkataraman
Mathematics Institute
University of Warwick
Zeeman Building
GB-Coventry CV4 7AL

Prof. Dr. Axel Voigt
Abteilung Mathematik
Technische Universität Dresden
Mommsenstr. 13
01069 Dresden

Dr. Valentina Vulcanov
Fachbereich Mathematik
Universität Potsdam
Am Neuen Palais 10
14469 Potsdam

Maren-Wanda Wolf
Institut für Mathematik II (WE2)
Freie Universität Berlin
Arnimallee 2-6
14195 Berlin

Prof. Dr. Harry Yserentant
Institut für Mathematik
Technische Universität Berlin
Straße des 17. Juni 136
10623 Berlin